10/537798

Figure 1. Energy storage triglyceride content of a Drosophila *fwd* (Gadfly Accession Number CG7004) mutant

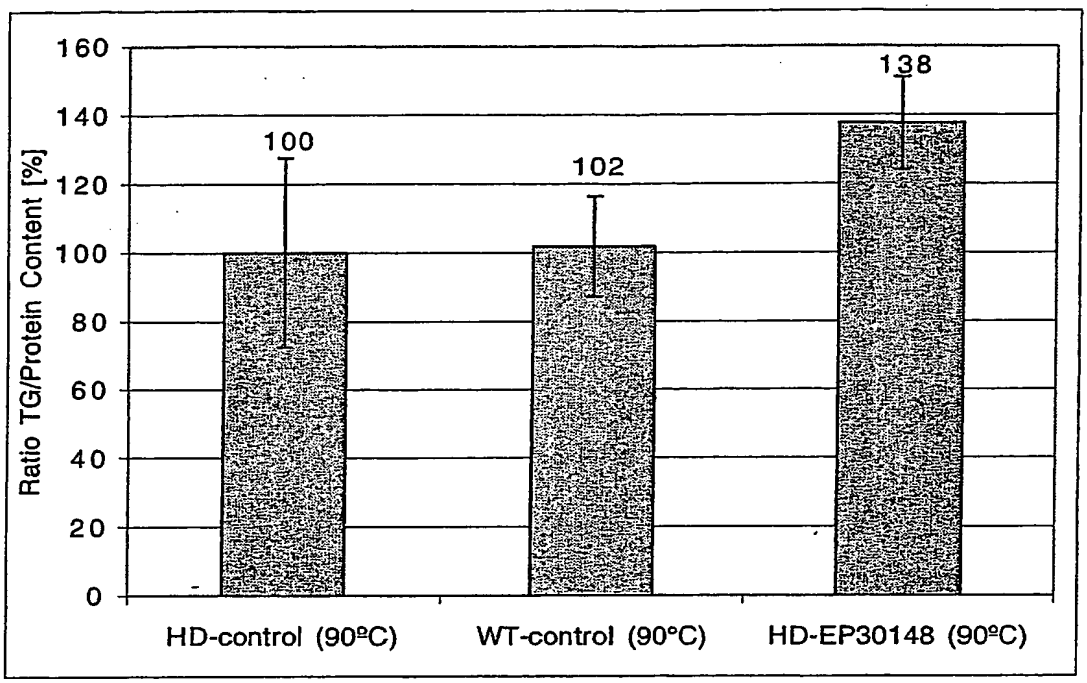

BEST AVAILABLE COPY

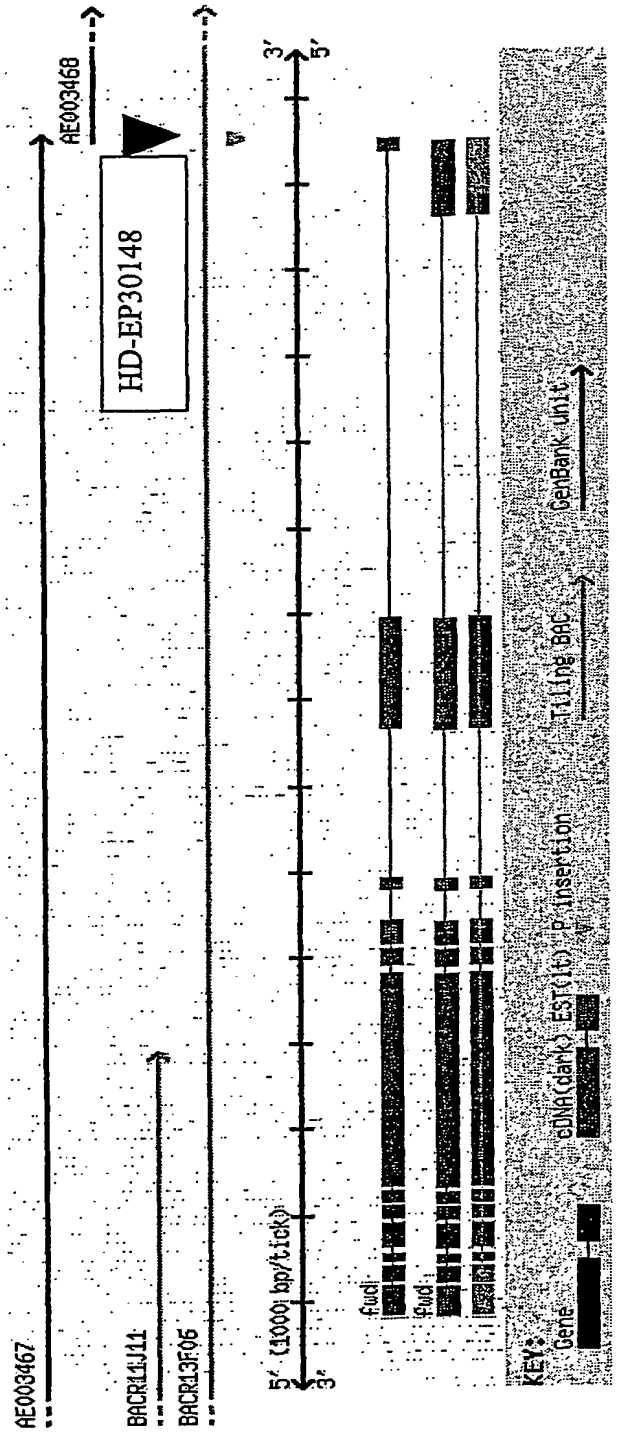

Figure 2. Molecular organization of the *fwd* gene (GadFly Acession Number CG7004)

10/537798

Figure 3. Expression of the *fwd* (GadFly Accession Number CG7004) Homolog in Mammalian Tissues

Figure 3A. Real-time PCR analysis of the catalytic beta polypeptide of phosphatidylinositol 4-kinase (Pik4cb) in wild type mouse tissues

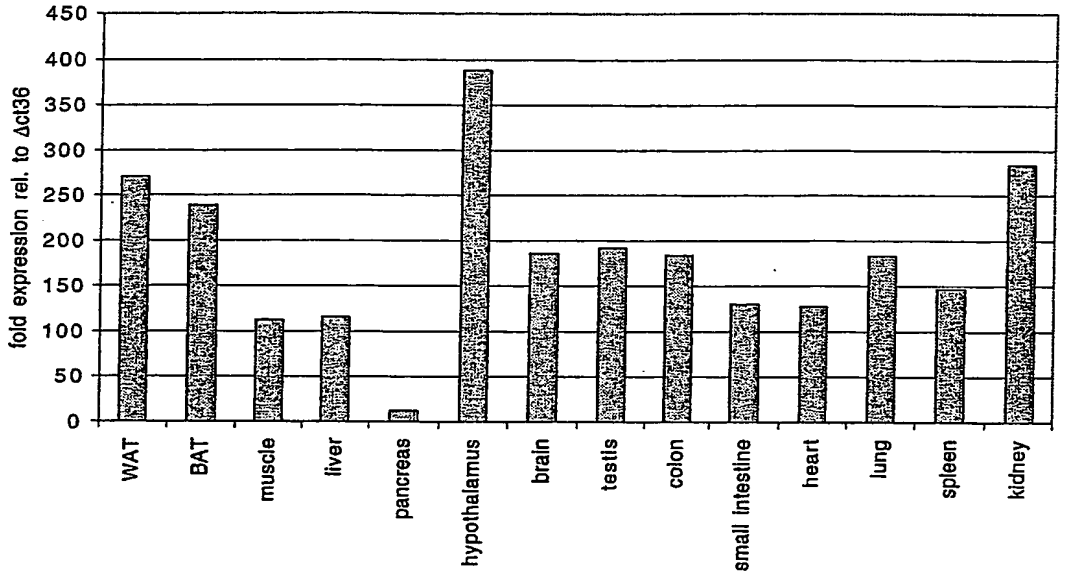

Figure 3B. Real-time PCR analysis of Pik4cb expression in different mouse models

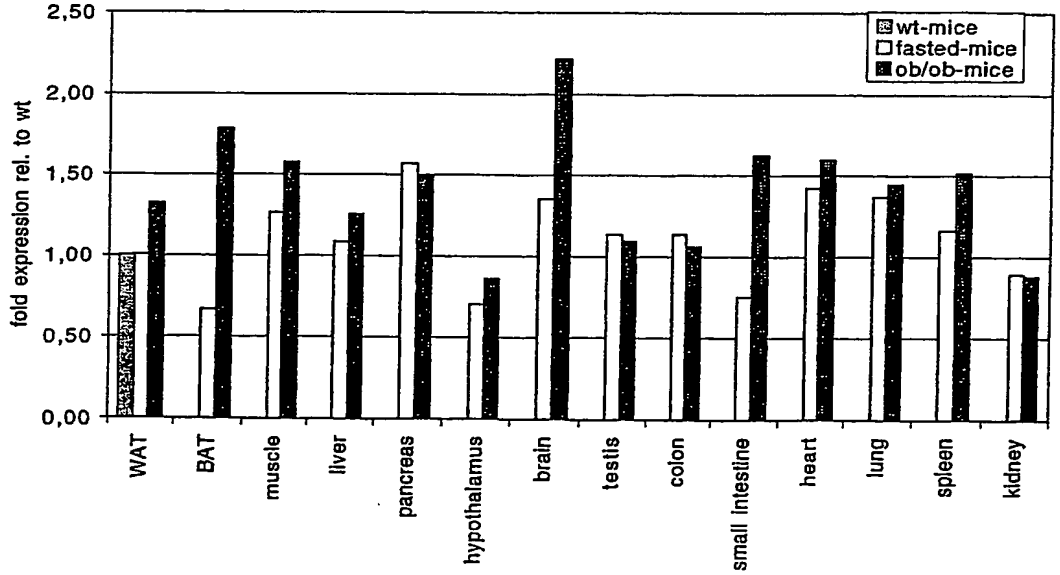

Figure 3C. Real-time PCR analysis of Pik4cb expression in mice fed with a high fat diet compared to mice fed with a control diet

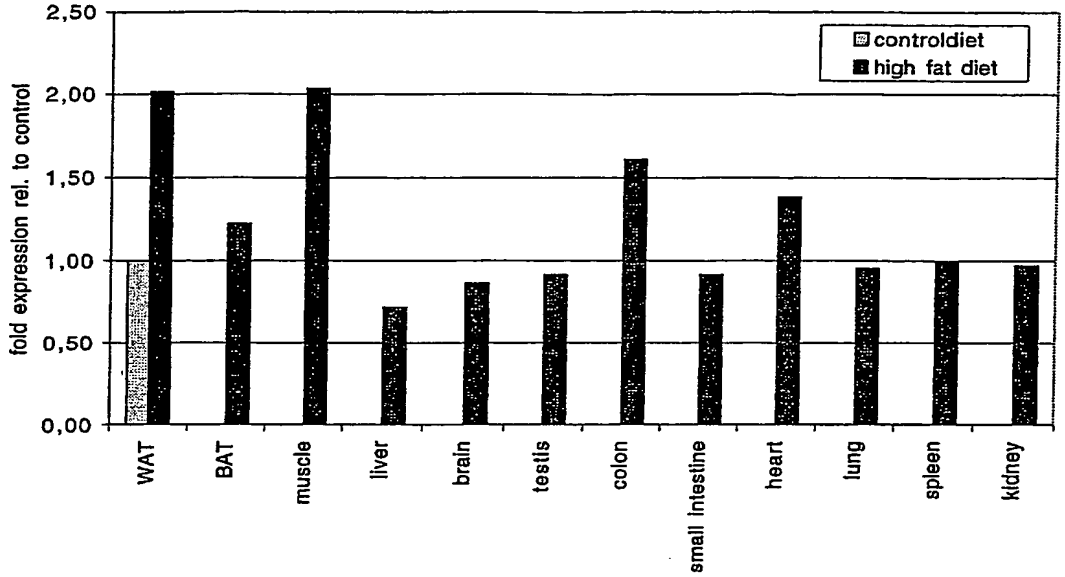

Figure 3D. Real-time PCR analysis of Pik4cb expression in 3T3-L1 cells differentiated from preadipocytes to mature adipocytes

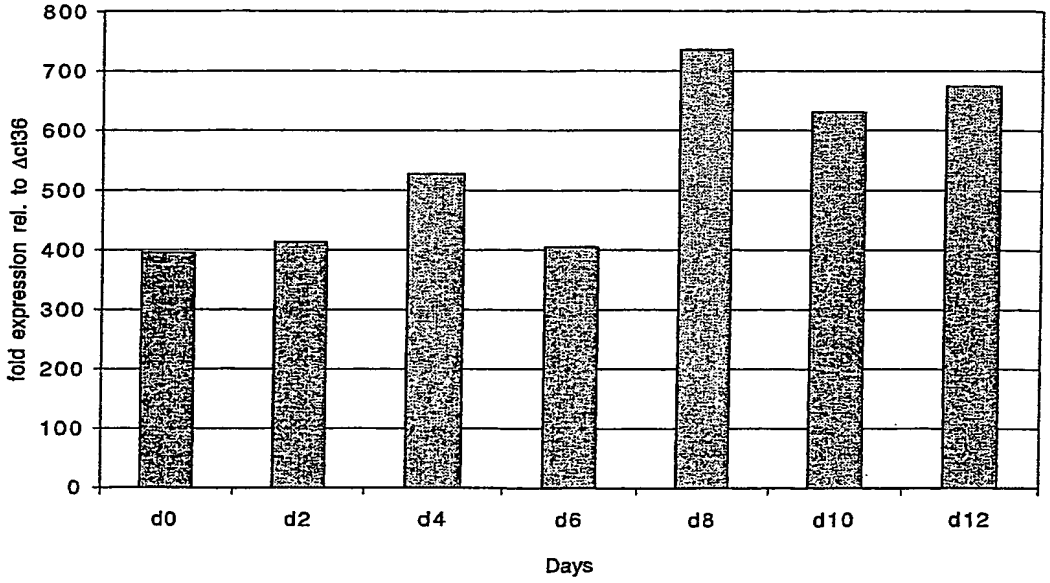

10/537798

Figure 4. Expression of the human *fwd* homolog in mammalian (human) tissue.

Figure 4A. Microarray analysis of phosphatidylinositol 4-kinase, catalytic, beta polypeptide (PIK4CB) expression in human abdominal derived primary adipocyte cells during the differentiation from preadipocytes to mature adipocytes

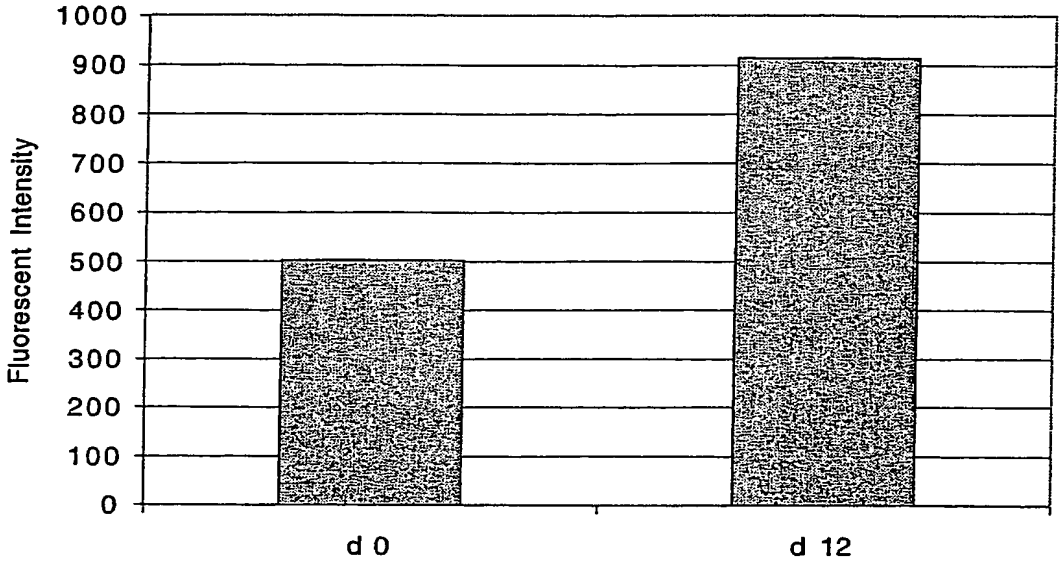

Figure 4B. Microarray analysis of PIK4CB expression in ahuman adipocyte cell line during the differentiation from preadipocytes to mature adipocytes

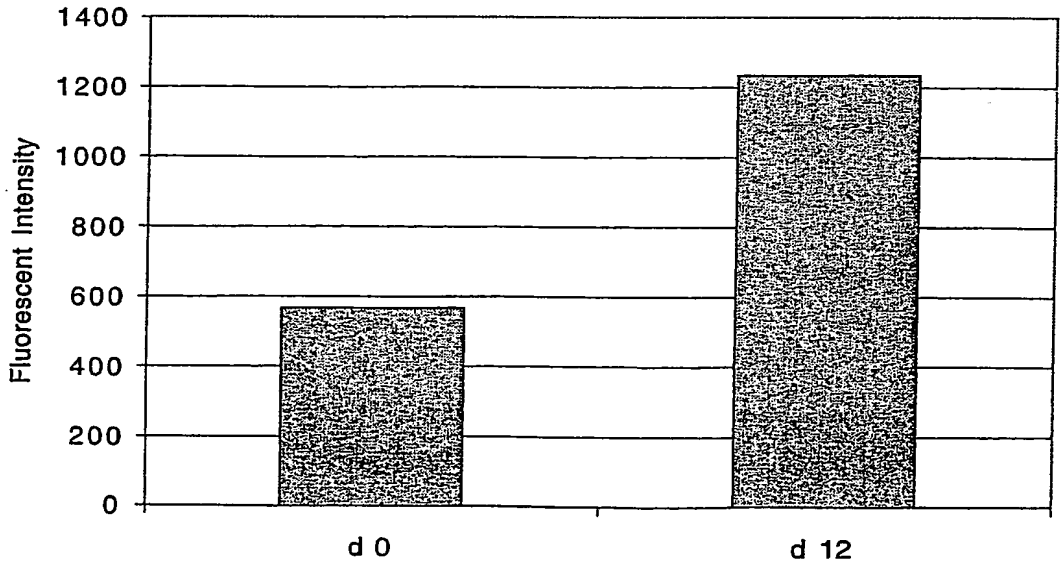

A01537798

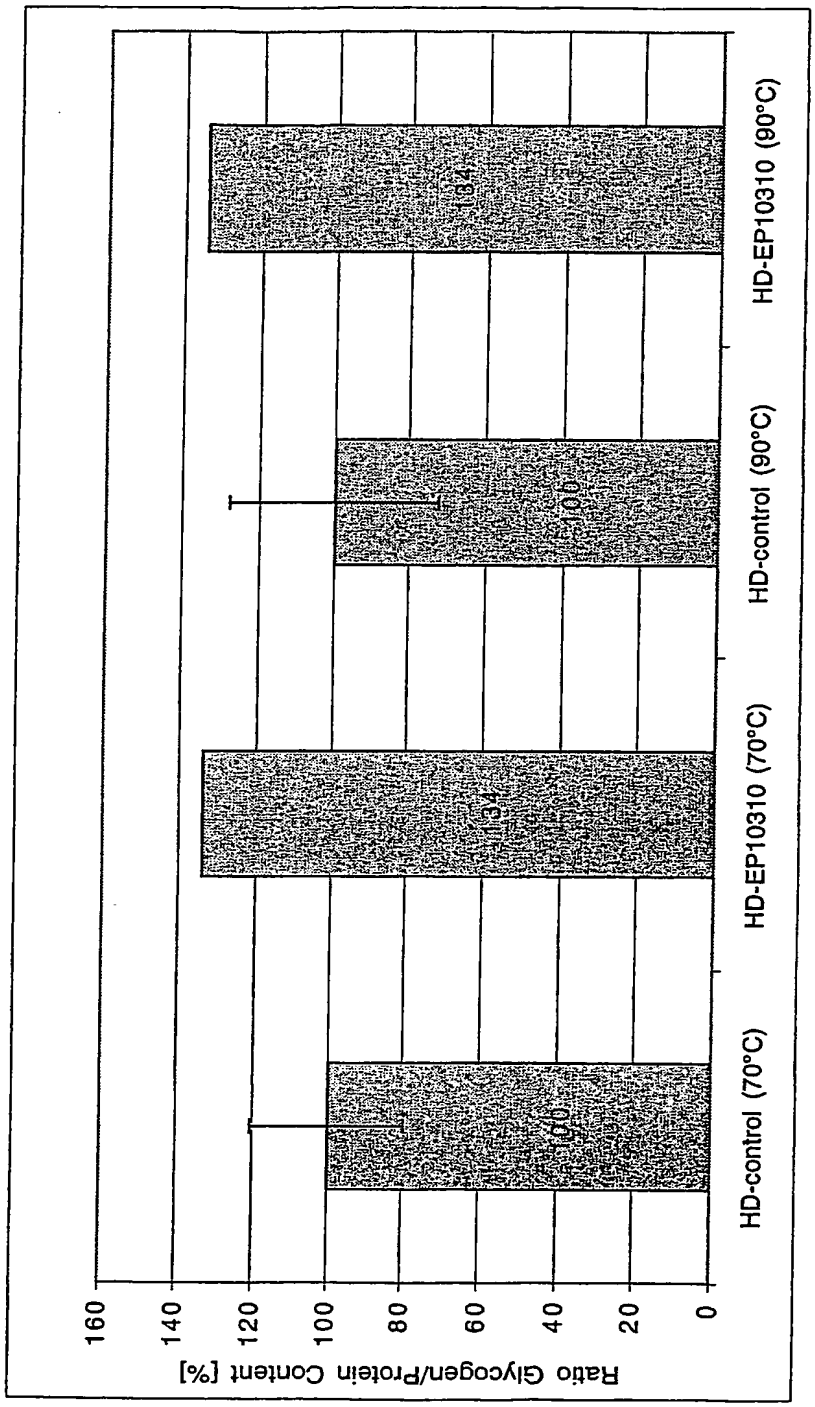

Figure 5. Glycogen content of a *Drosophila protein phosphatase 2C (Pp2C1*; GadFly Accession Number CG2984) mutant

10/537798

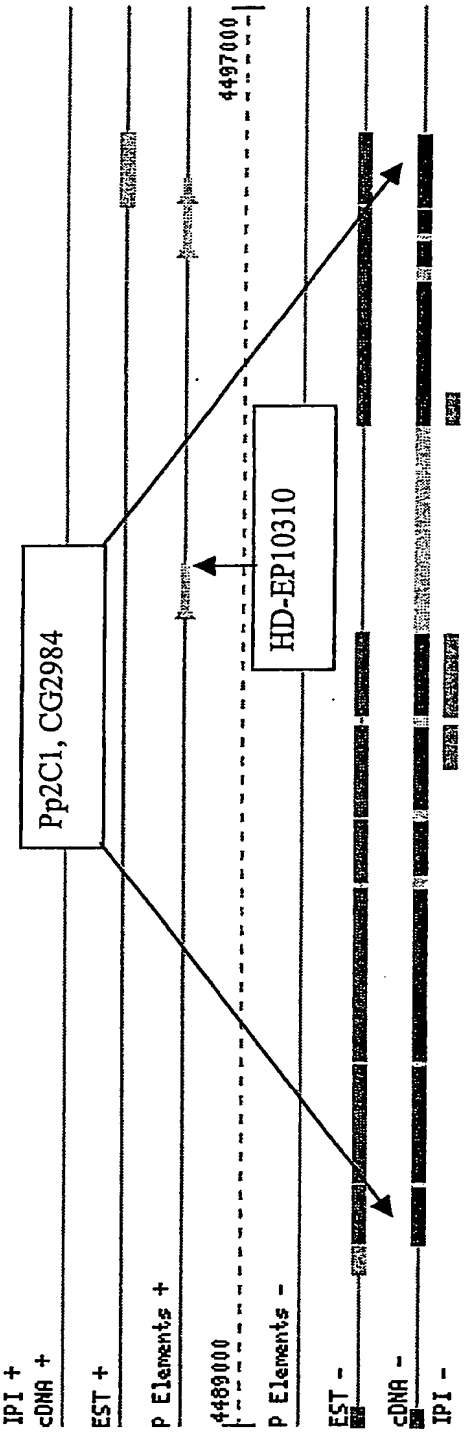

Figure 6. Molecular organization of the *Pp2C1* gene (GadFly Acession Number CG2984)

10/537798

Figure 7. Expression of the *Pp2C1* (GadFly Accession Number CG2984) Homolog in Mammalian Tissues

Figure 7A. Real-time PCR analysis of protein phosphatase 1D magnesium-dependent, delta isoform (Ppm1d) in wild type mouse tissues

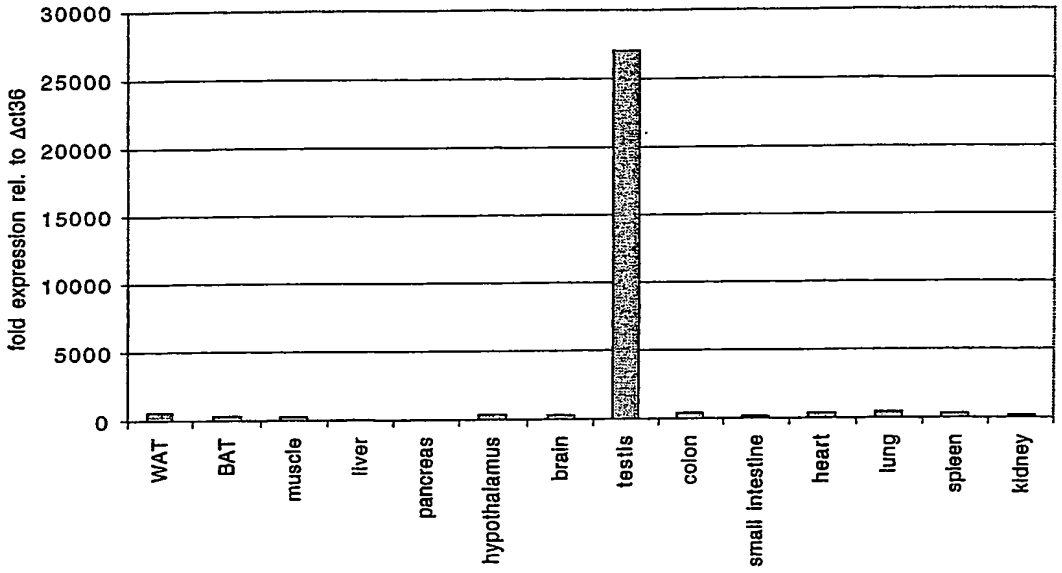

Figure 7B. Real-time PCR analysis of Ppm1d expression in different mouse models

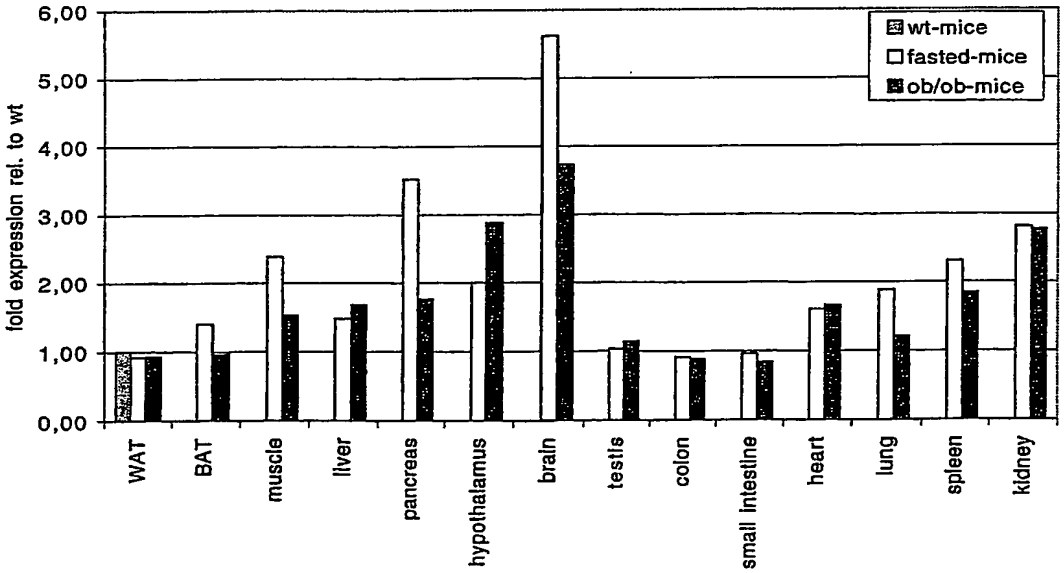

10/537798

Figure 7C. Real-time PCR analysis of Ppm1d expression in mice fed with a high fat diet compared to mice fed with a control diet

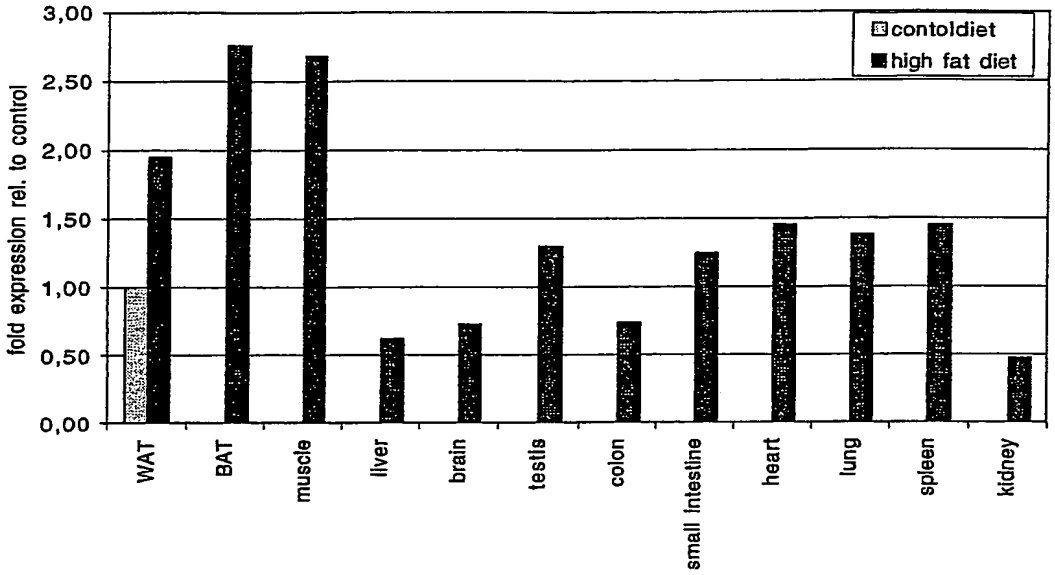

Figure 7D. Real-time PCR analysis of Ppm1d expression in 3T3-L1 cells differentiated from preadipocytes to mature adipocytes

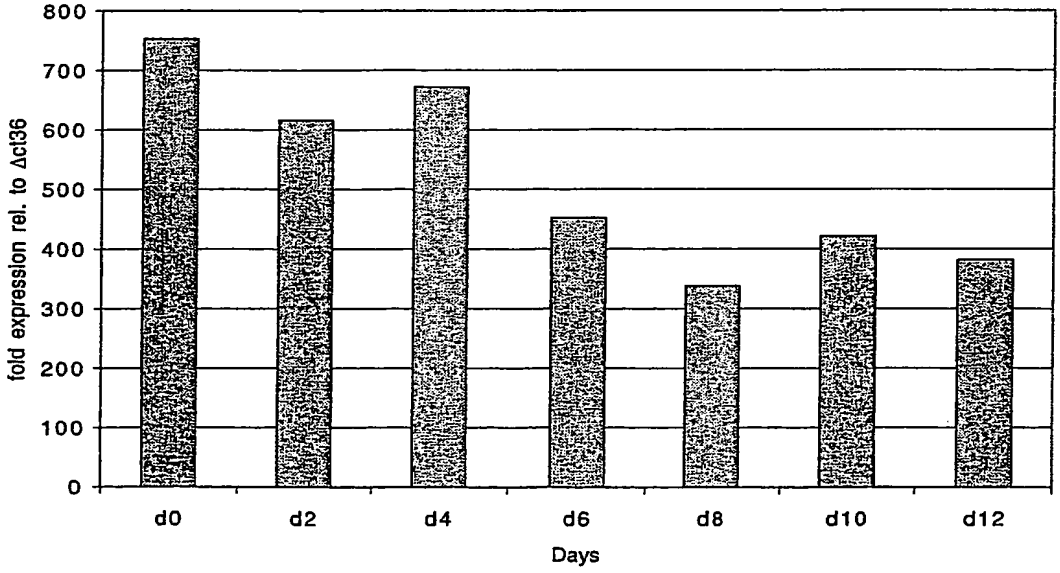

10/537798

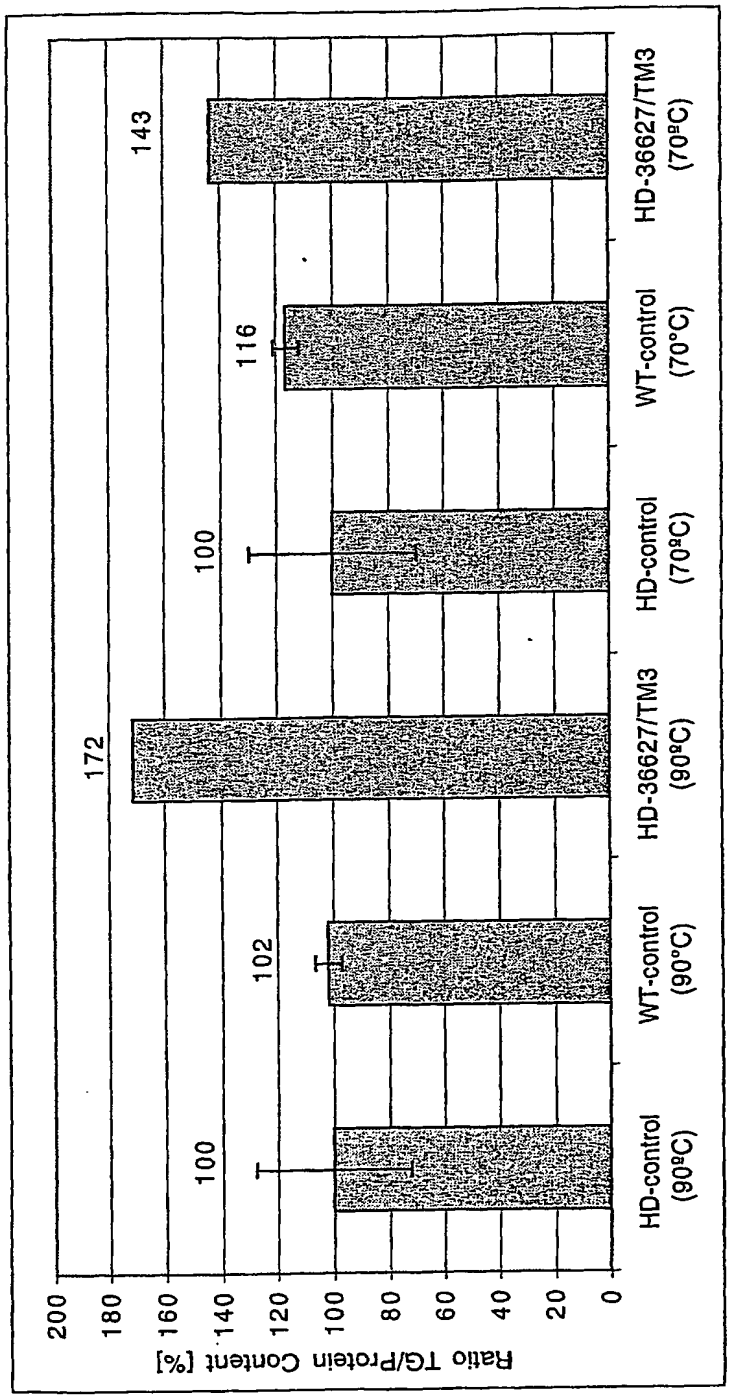

Figure 8. Energy storage triglyceride content of a Drosophila *Adk3* mutant (Gadfly Acc. No. CG6612)

10/537798

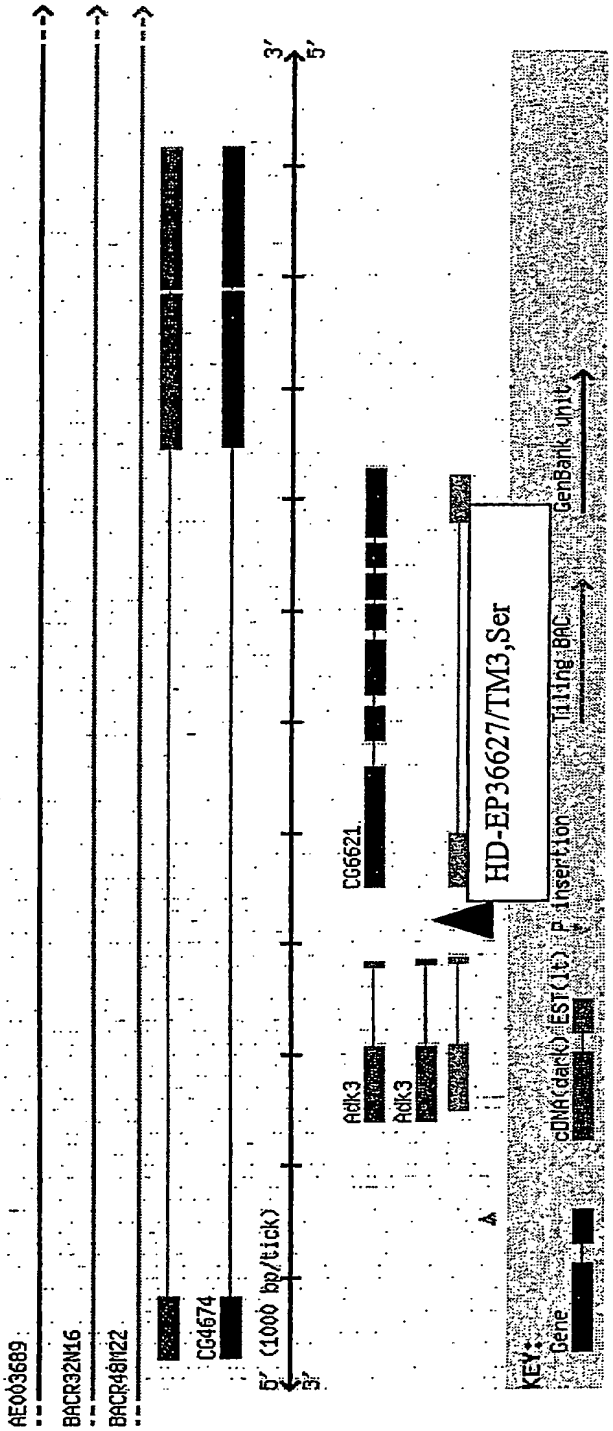

Figure 9. Molecular organization of the *Adk3* gene (GadFly Acession Number CG6612)

10/537798

Figure 10. Expression of *Adk3* (GadFly Accession Number CG6612) Homologs in Mammalian Tissues

Figure 10A. Real-time PCR analysis of adenylate kinase 3 alpha like (Akl3l) in wild type and control-diet mouse tissues

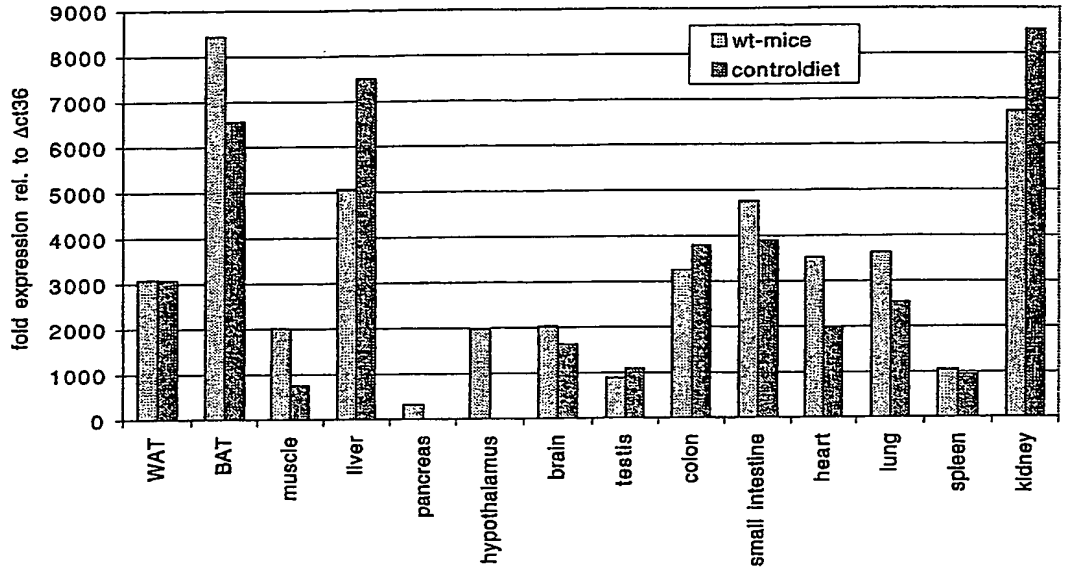

Figure 10B. Real-time PCR analysis of Akl3l expression in different mouse models and in mice fed with a high fat diet compared to mice fed with a control diet

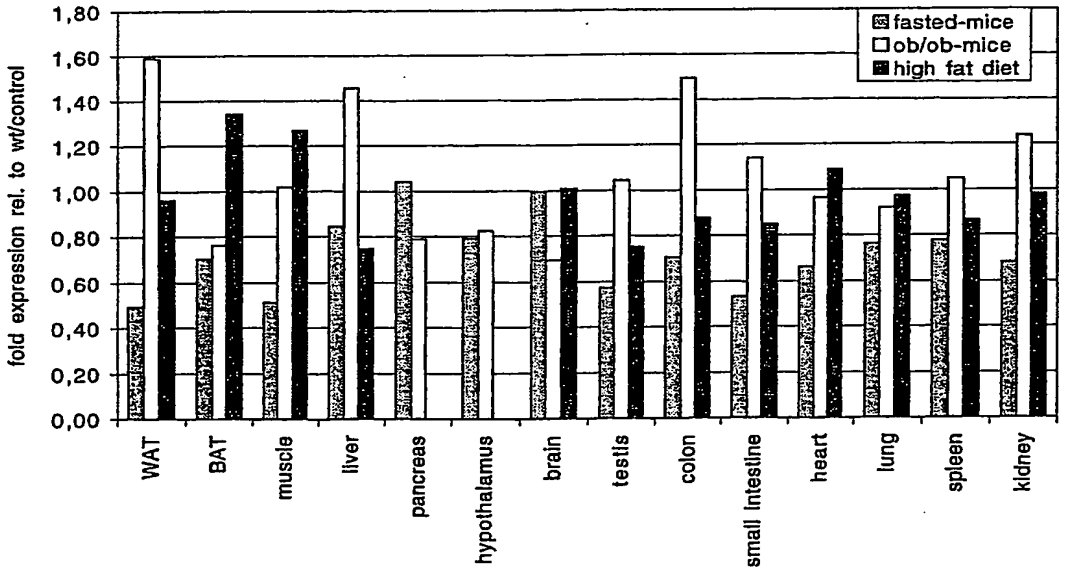

Figure 10C. Real-time PCR analysis of Akl3l expression in 3T3-L1 cells differentiated from preadipocytes to mature adipocytes

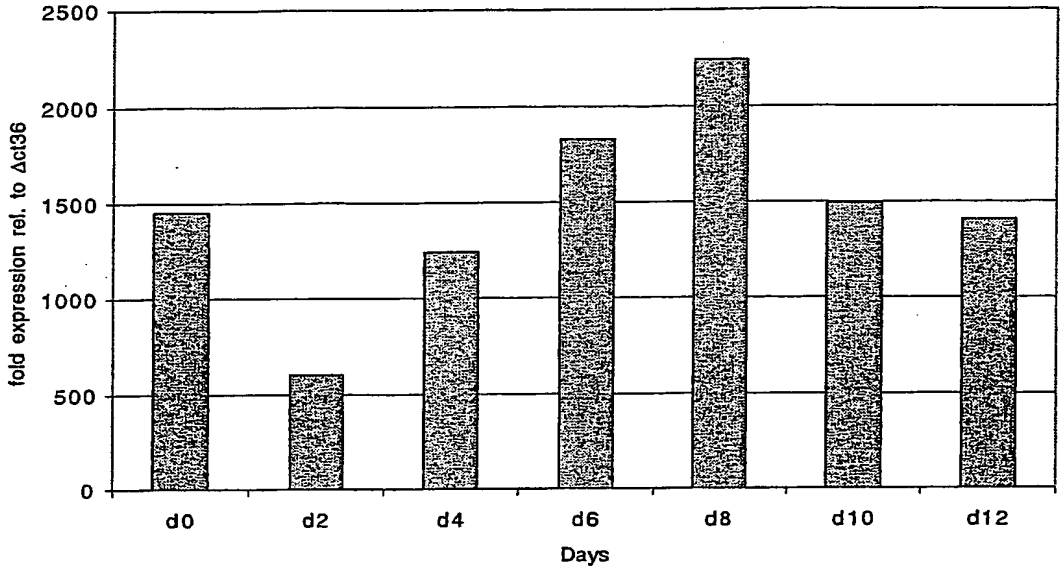

Figure 10D. Real-time PCR analysis of adenylate kinase 4 (Ak4) in wild type and control-diet mouse tissues

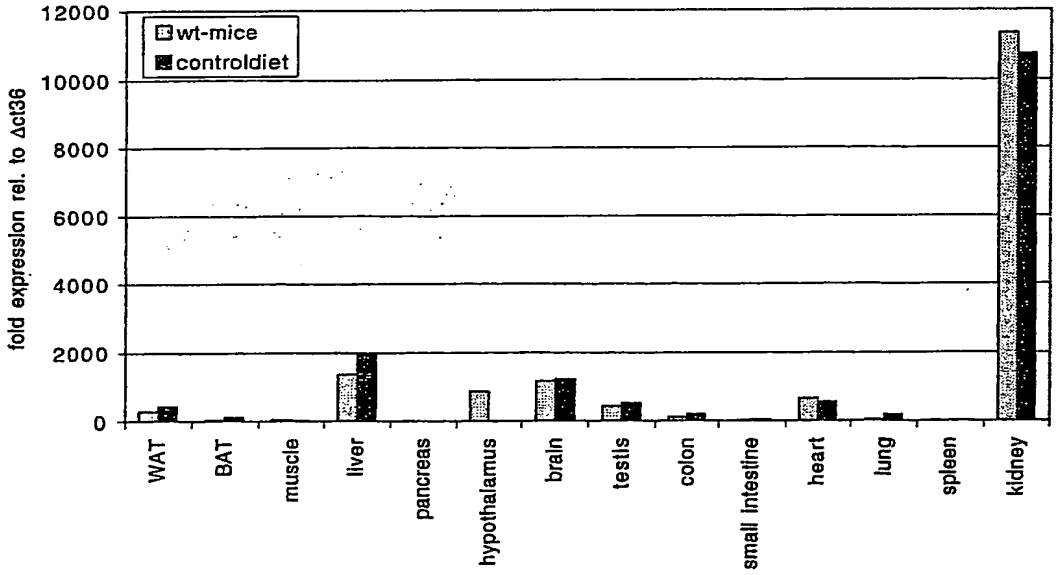

10/537798

Figure 10E. Real-time PCR analysis of Ak4 expression in different mouse models and in mice fed with a high fat diet compared to mice fed with a control diet

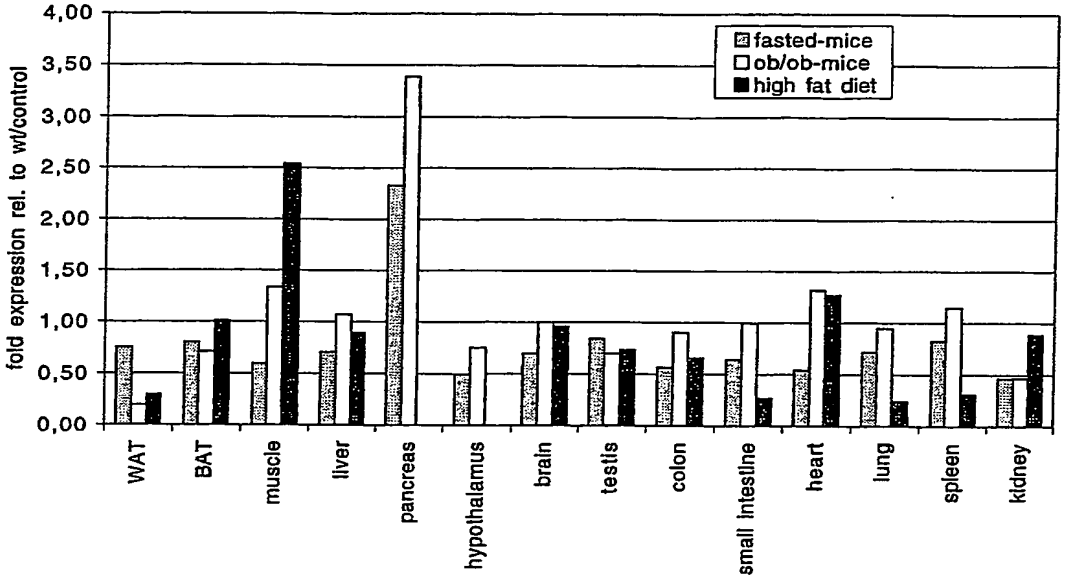

Figure 10F. Real-time PCR analysis of Ak4 expression in 3T3-L1 cells differentiated from preadipocytes to mature adipocytes

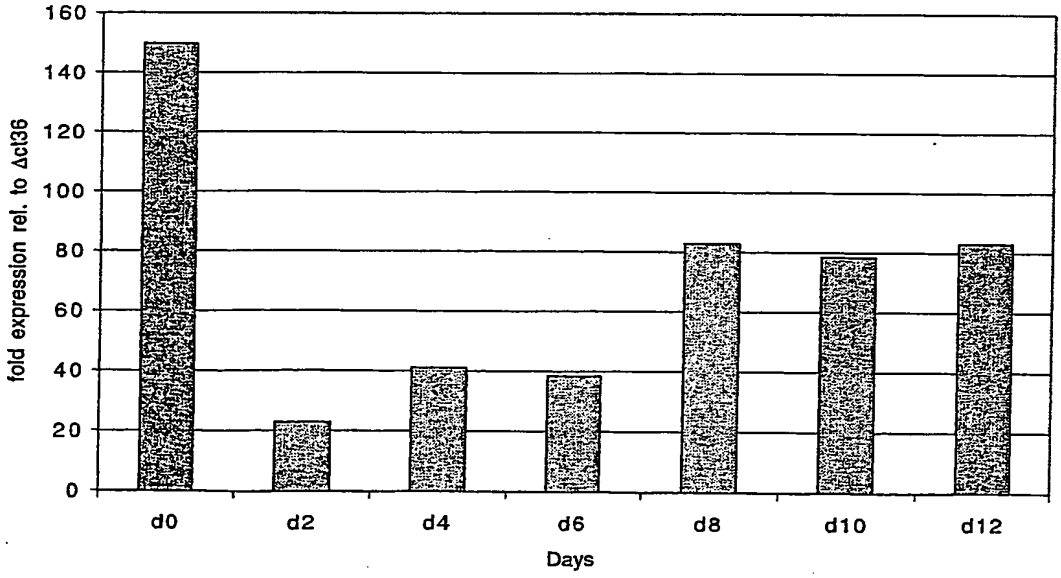

10/537798

Figure 11. Expression of human *Adk3* homologs in mammalian (human) tissue.

Figure 11A. Microarray analysis of adenylate kinase 3 like 1 (AK3L1) expression in human abdominal derived primary adipocyte cells during the differentiation from preadipocytes to mature adipocytes

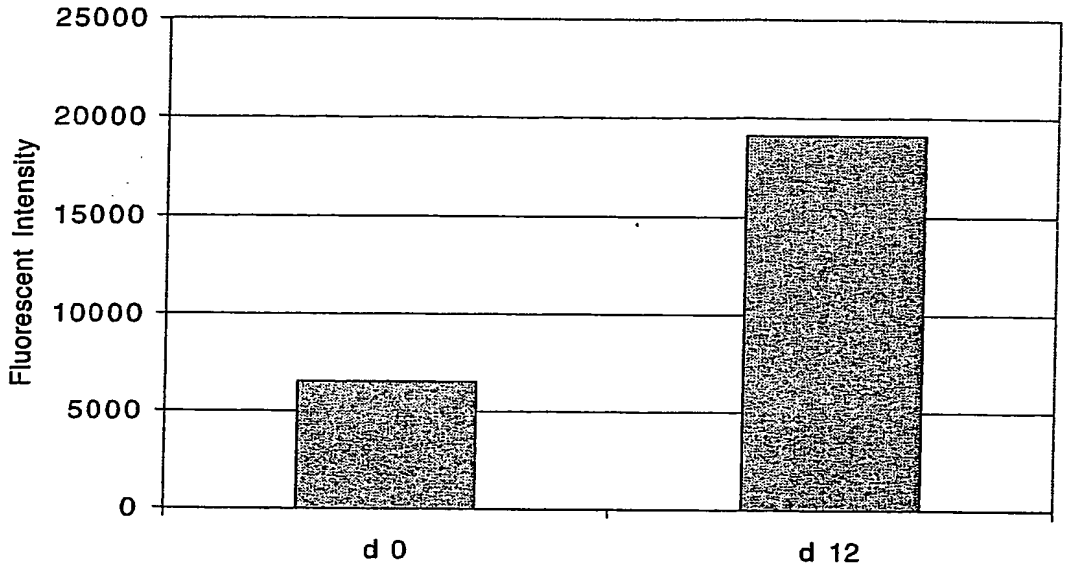

Figure 11B. Microarray analysis of adenylate kinase 3 (AK3) expression a human adipocyte cell line during the differentiation from preadipocytes to mature adipocytes

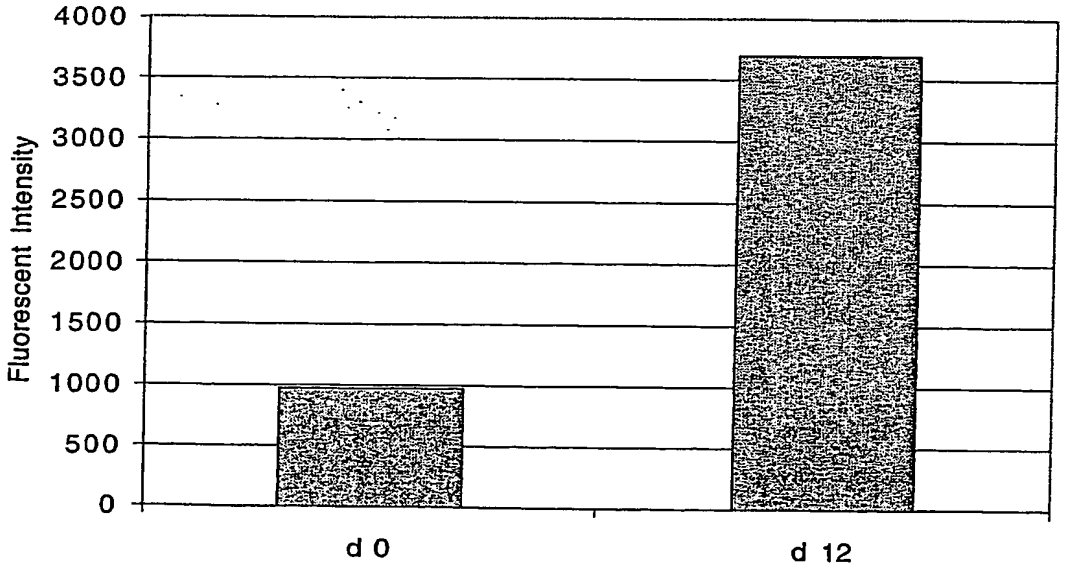

10/537798

Figure 12. Energy storage triglyceride content of a Drosophila CG3860 (Gadfly Accession Number) mutant

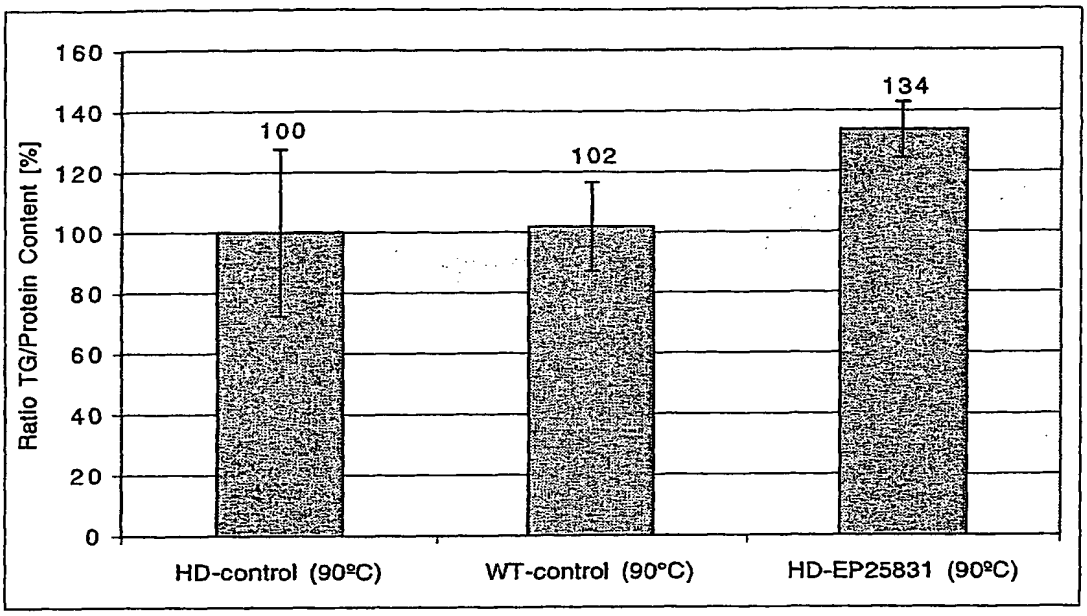

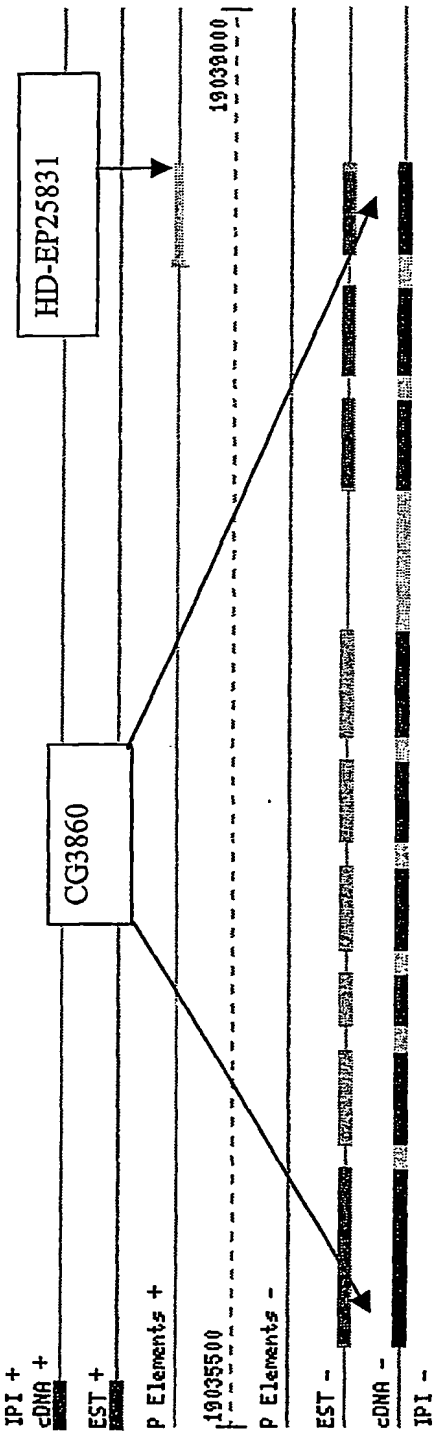

Figure 13. Molecular organization of the CG3860 gene (GadFly Acession Number)

10/537798

Figure 14. Expression of the CG3860 (GadFly Accession Number) Homologs in Mammalian Tissues

Figure 14A. Real-time PCR analysis of oxysterol binding protein-like 1A (Osbpl1a) expression in wild type and control-diet mouse tissues

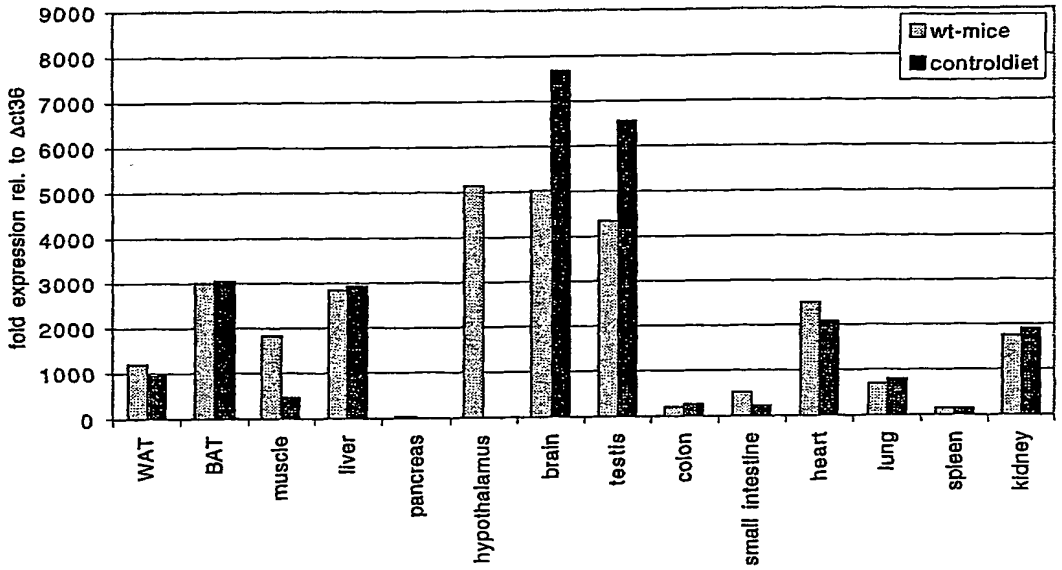

Figure 14B. Real-time PCR analysis of Osbpl1a expression in different mouse models and in mice fed with a high fat diet compared to mice fed with a control diet

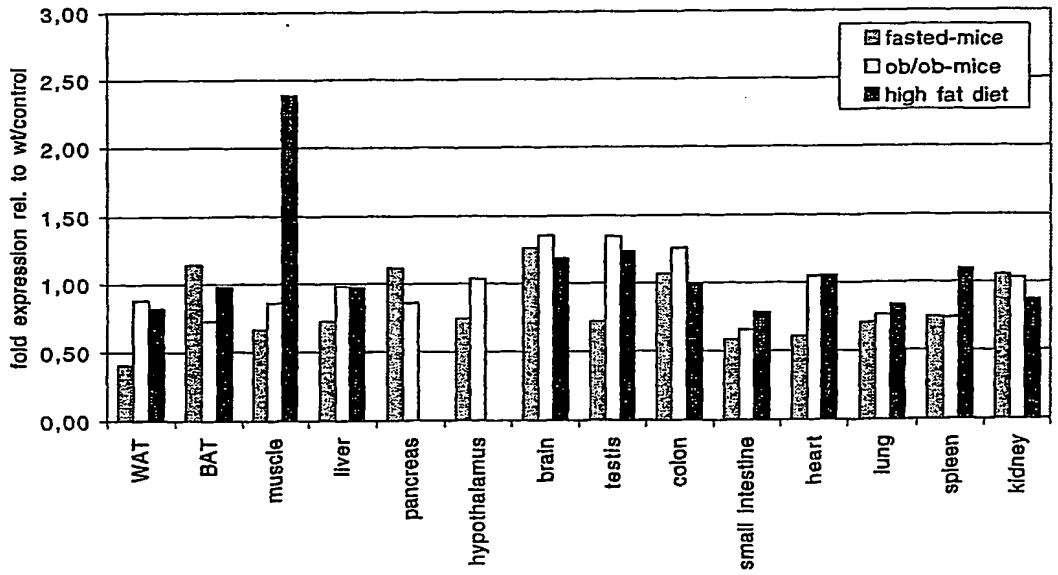

Figure 14C. Real-time PCR analysis of Osbpl1a expression in 3T3-L1 cells differentiated from preadipocytes to mature adipocytes

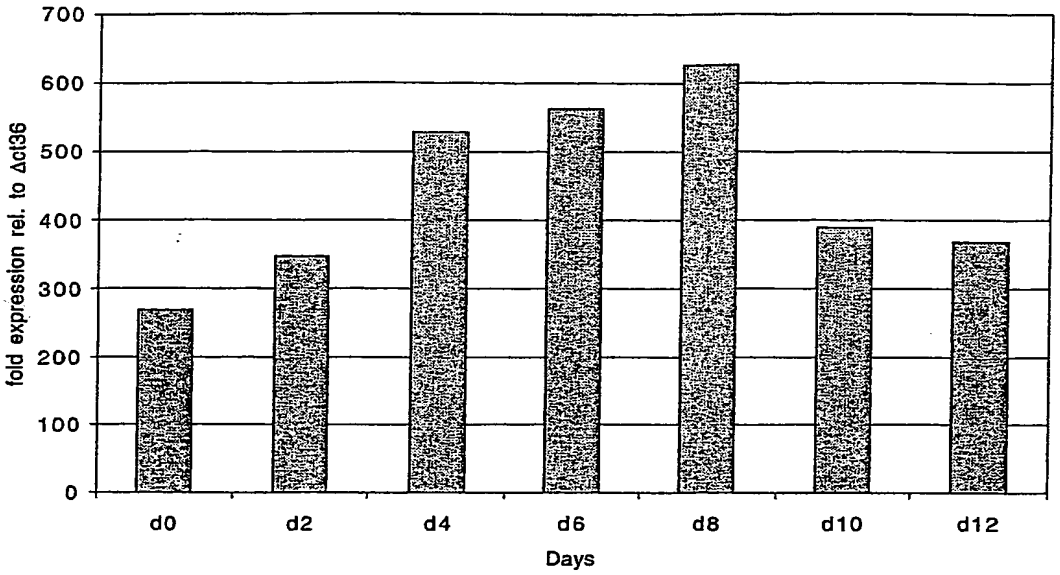

Figure 14D. Real-time PCR analysis of oxysterol binding protein-like 2 (Osbpl2) expression in wild type and control-diet mouse tissues

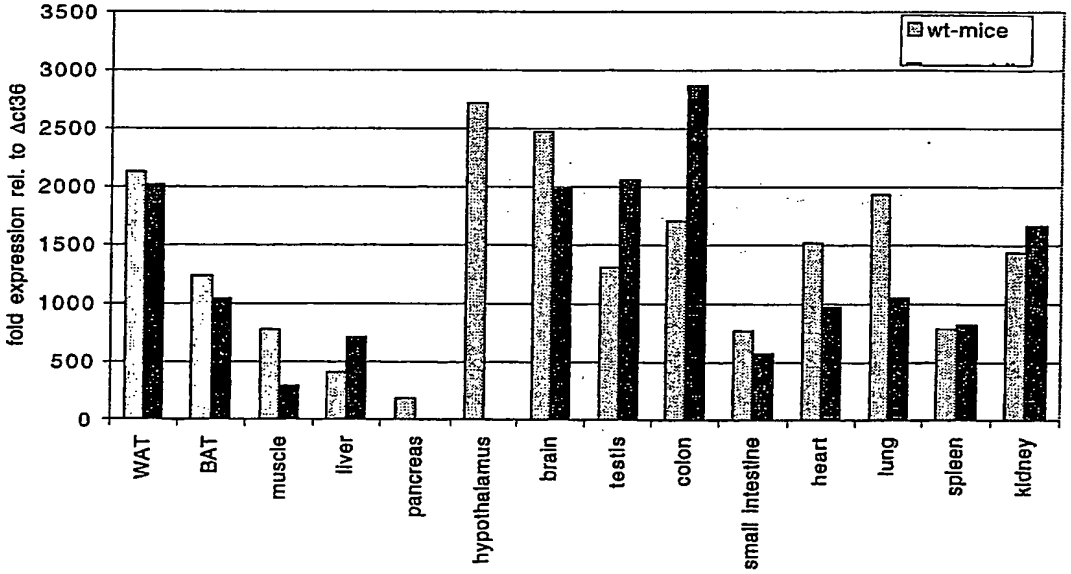

10/537798

Figure 14E. Real-time PCR analysis of Osbpl2 expression in different mouse models and in mice fed with a high fat diet compared to mice fed with a control diet

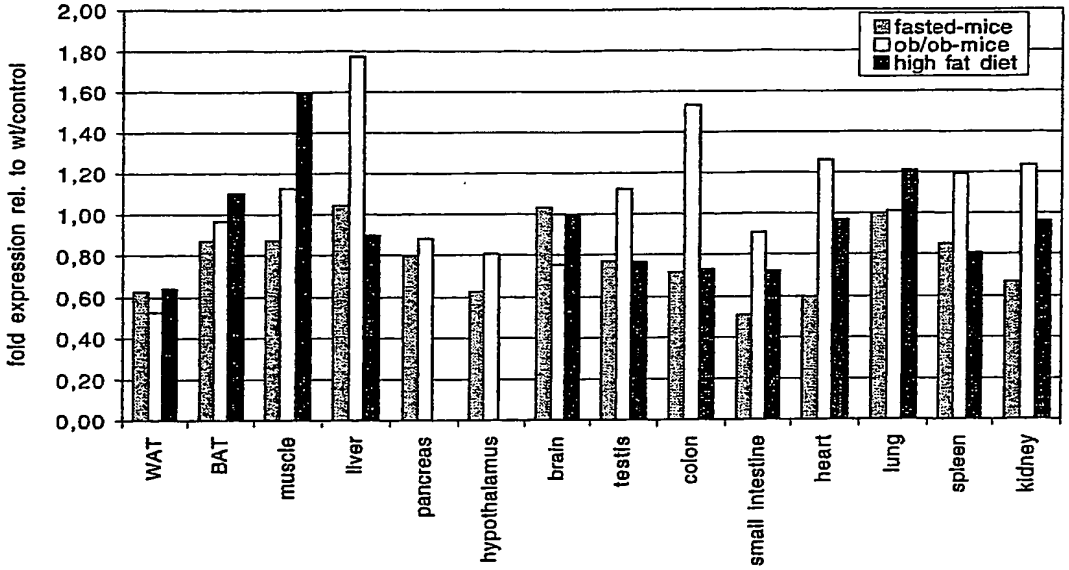

Figure 14F. Real-time PCR analysis of Osbpl2 expression in 3T3-L1 cells differentiated from preadipocytes to mature adipocytes

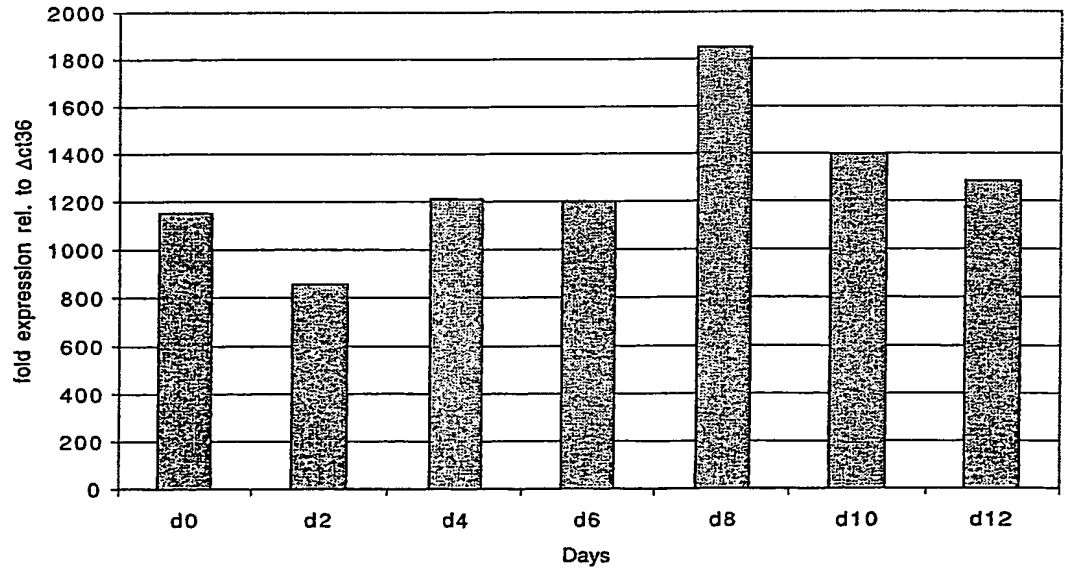

10/537798

Figure 15. Expression of human CG3860 (GadFly Accession Number) homologs in mammalian (human) tissue.

Figure 15A. Microarray analysis of oxysterol binding protein-like 1A (OSBPL1A) expression in human abdominal derived primary adipocyte cells during the differentiation from preadipocytes to mature adipocytes

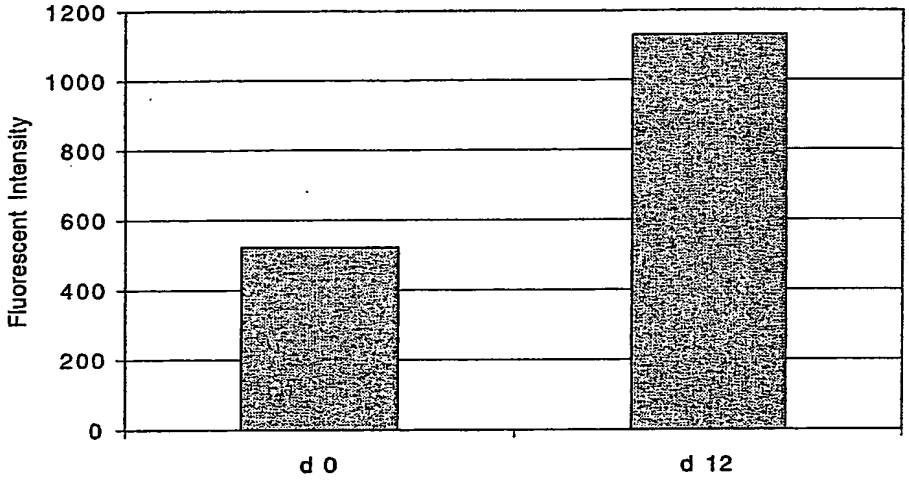

Figure 15B. Microarray analysis of oxysterol binding protein-like 1A (OSBPL1A) expression in a human adipocyte cell line during the differentiation from preadipocytes to mature adipocytes

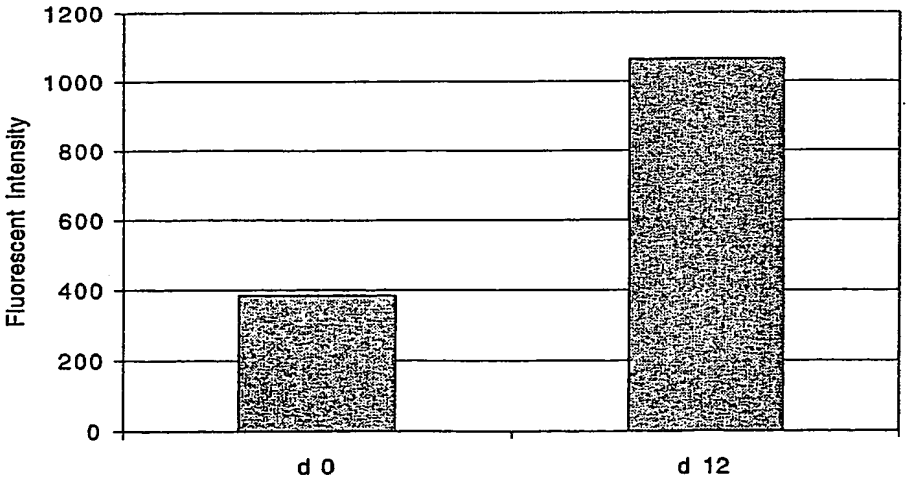

AU 2537798

Figure 15C. Microarray analysis of oxysterol binding protein-like 2 (OSBPL2) expression in a human adipocyte cell line during the differentiation from preadipocytes to mature adipocytes

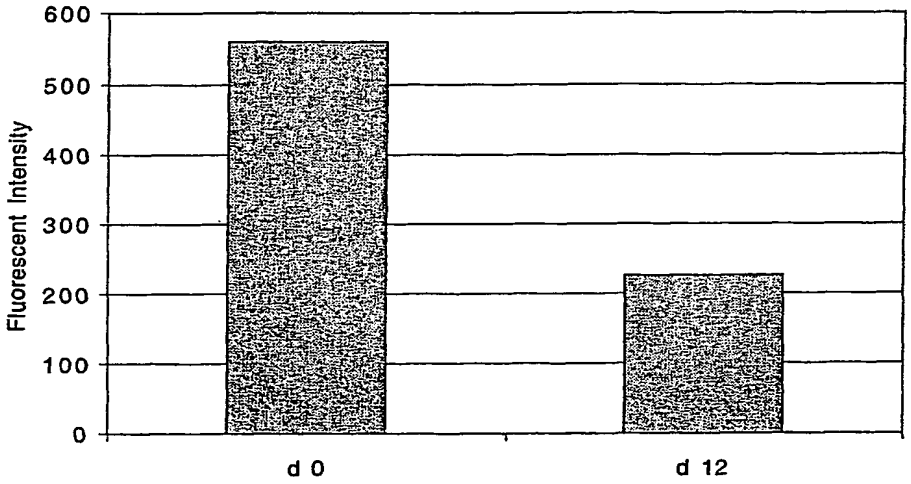

10/537798

Figure 16. Energy storage metabolite content of a Drosophila *Cdk4* mutant

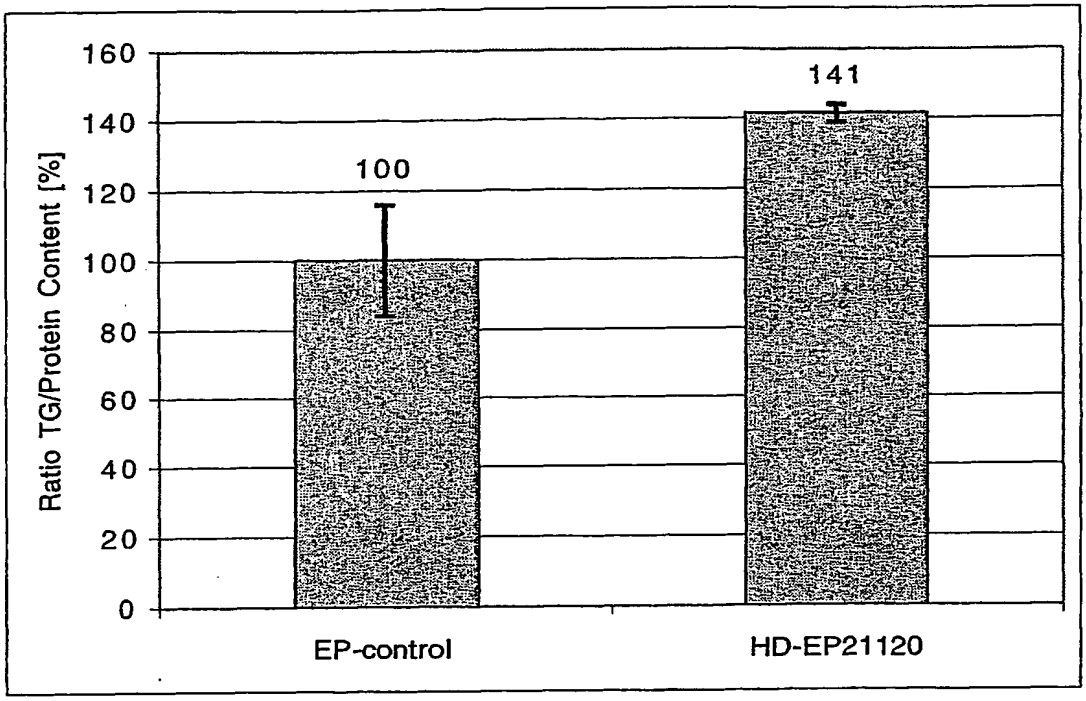

10/537798

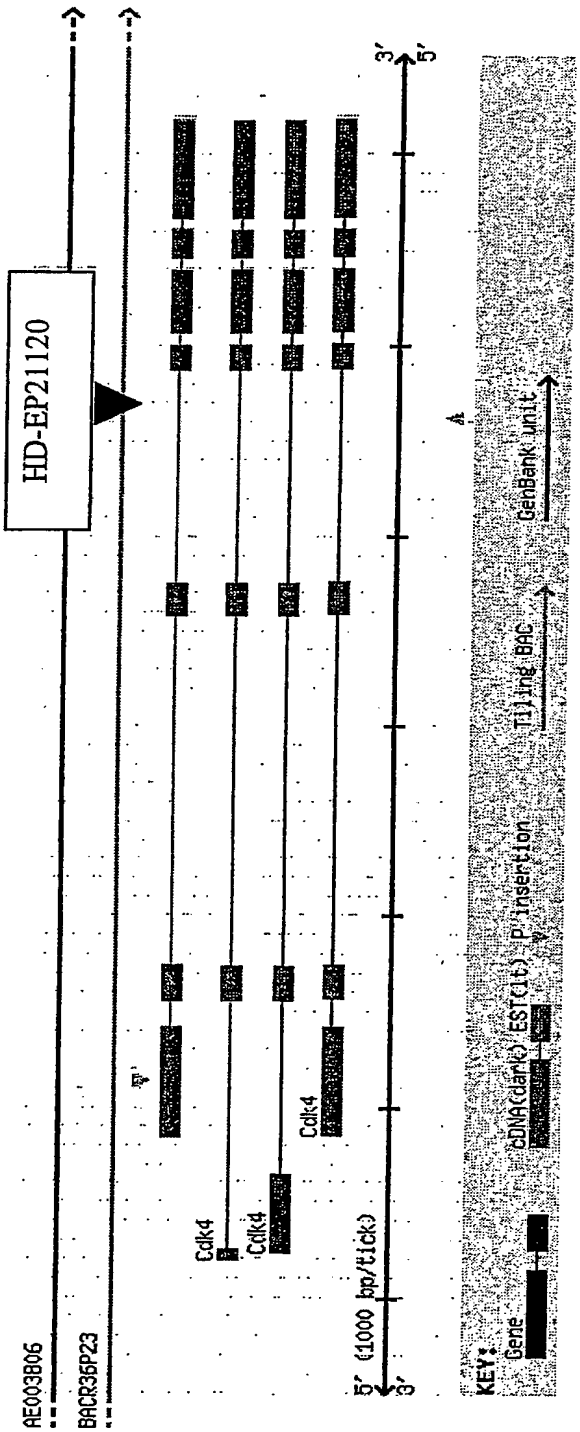

Figure 17. Molecular organization of the *Cdk4* gene (GadFly Acession Number CG5072)

10/537798

Figure 18. Energy storage metabolite content of a Drosophila CG7134 (Gadfly Accession Number) mutant

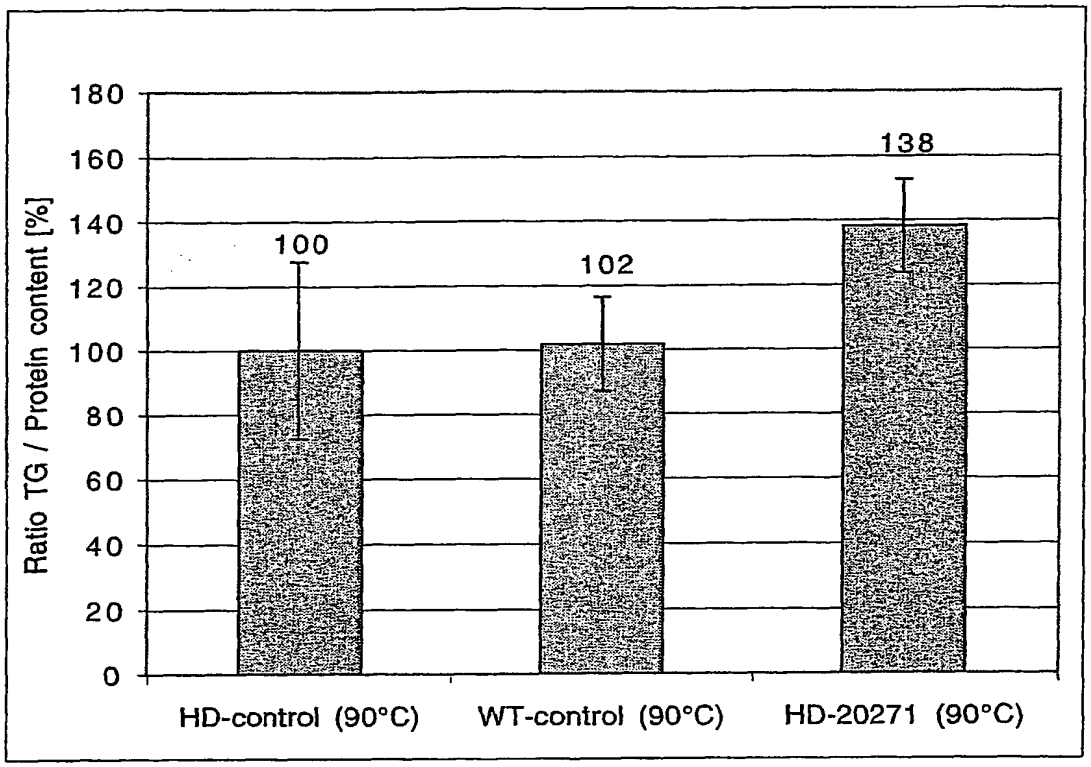

10/537798

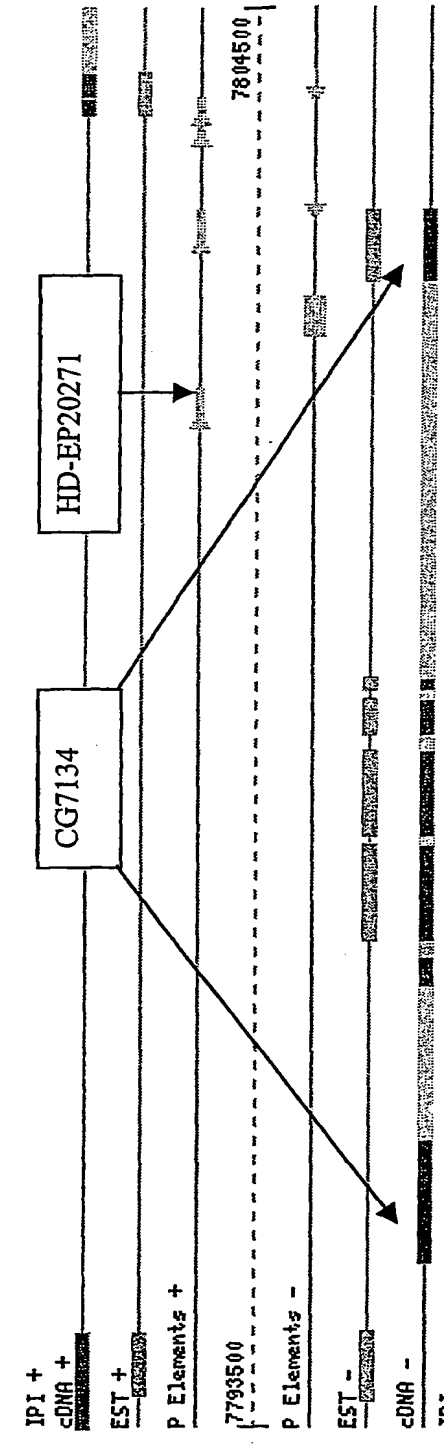

Figure 19. Molecular organization of the CG7134 gene (GadFly Acession Number)

10/537798

Figure 20. Energy storage metabolite content of a Drosophila *Eip75B* mutant

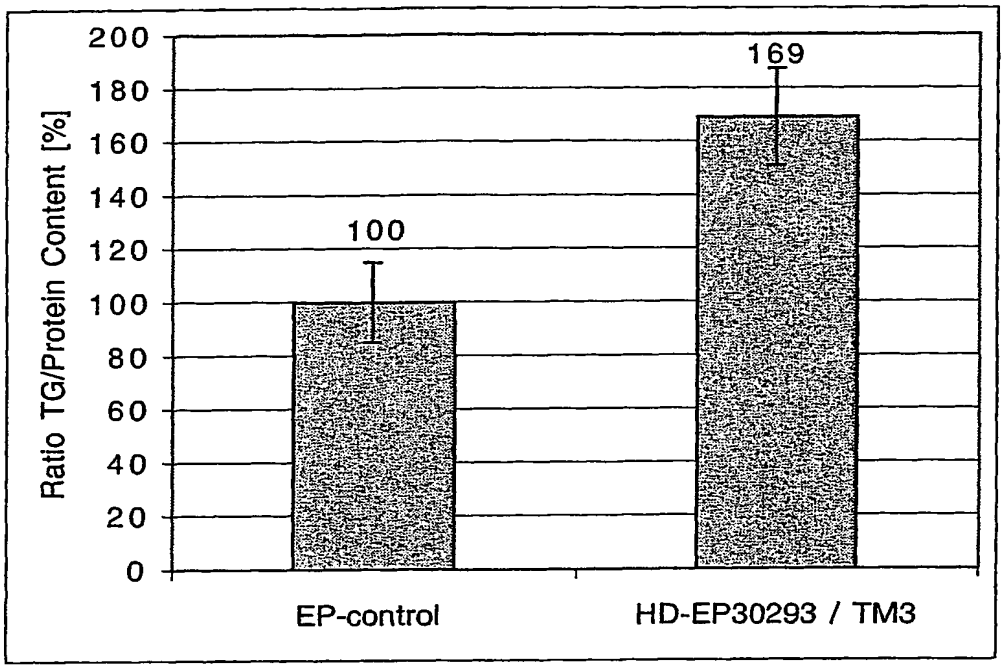

10/537798

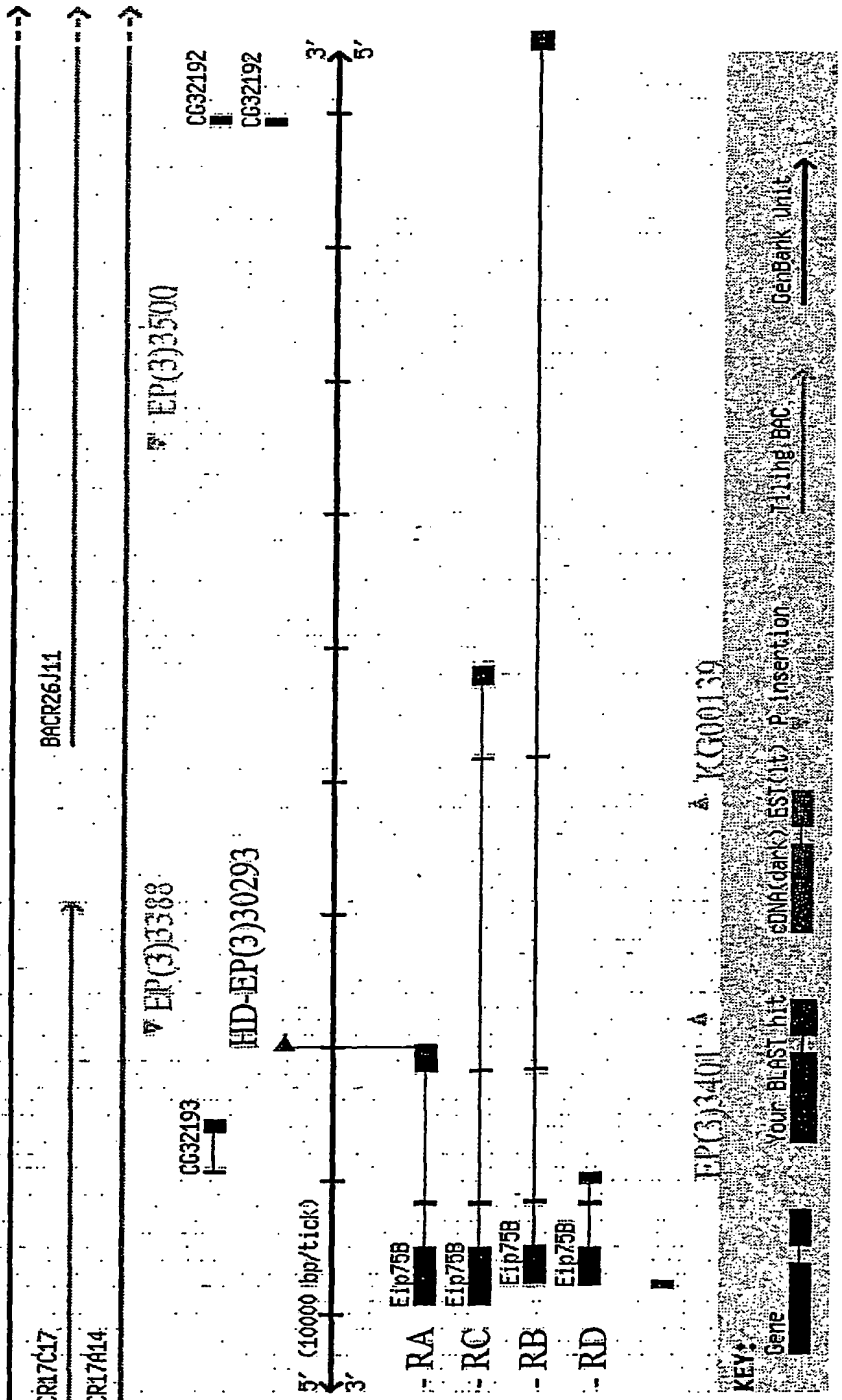

Figure 21. Molecular organization of the *Eip75B* gene (GadFly Acession Number CG8127)

Figure 22. Expression of tyrosine-protein kinases Nr1d1 and Nr1d2 in mammalian tissues

Figure 22A. Real-time PCR analysis of Nr1d1 expression in wildtype mouse tissues (ΔCt (pancreas) = 36)

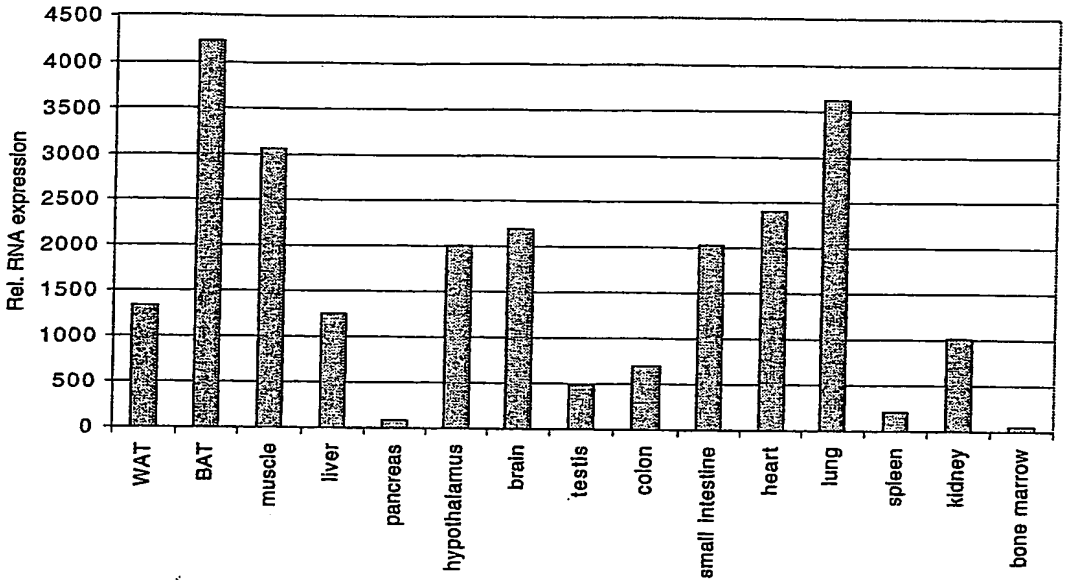

Figure 22B. Real-time PCR analysis of Nr1d1 expression in different mouse models

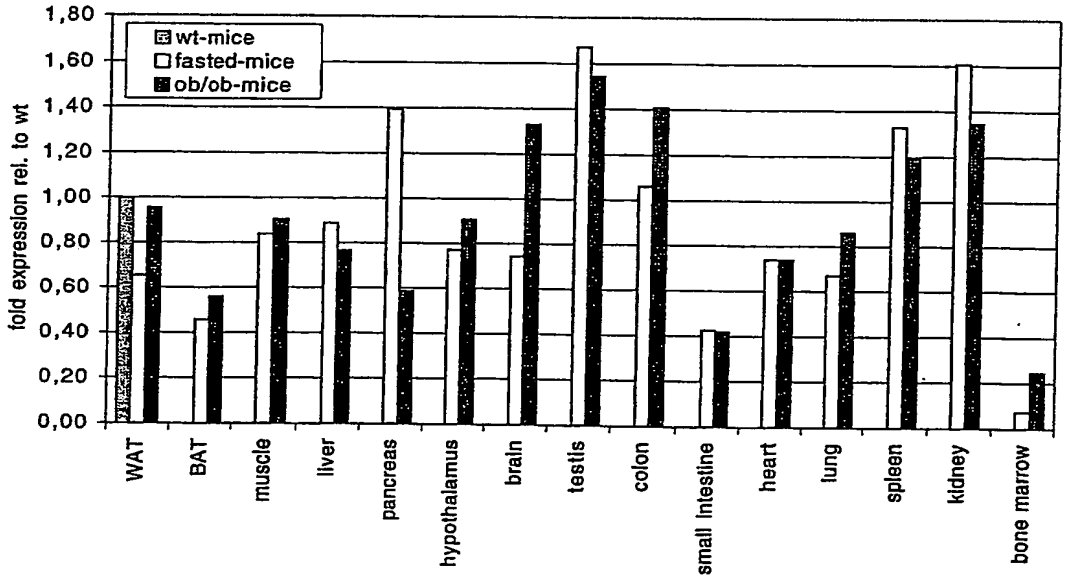

Figure 22C. Real-time PCR mediated analysis of Nr1d1 expression in 3T3-L1 cells differentiated from preadipocytes to mature adipocytes

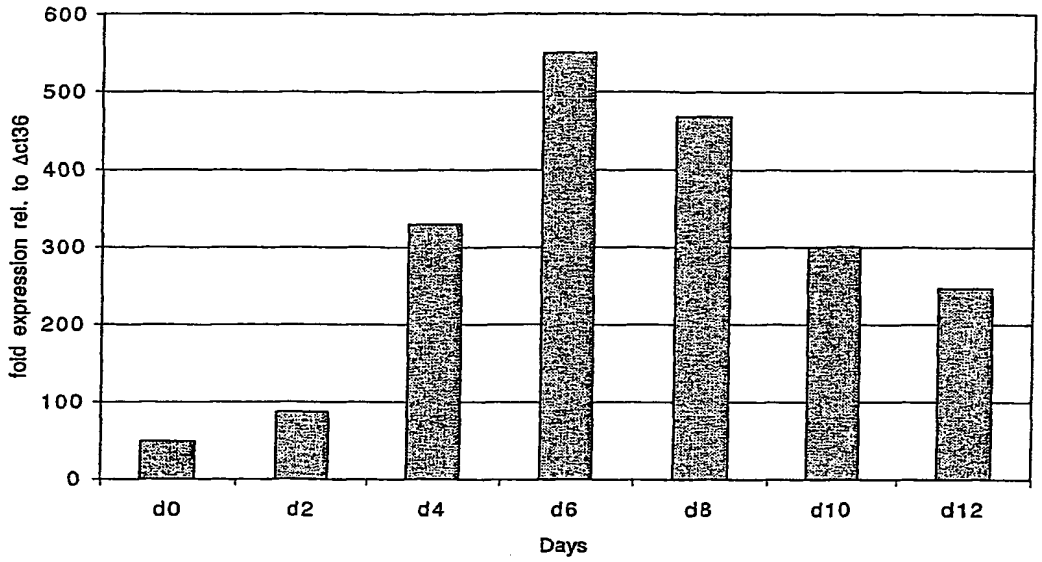

Figure 22D. Real-time PCR analysis of Nr1d2 expression in wildtype mouse tissues

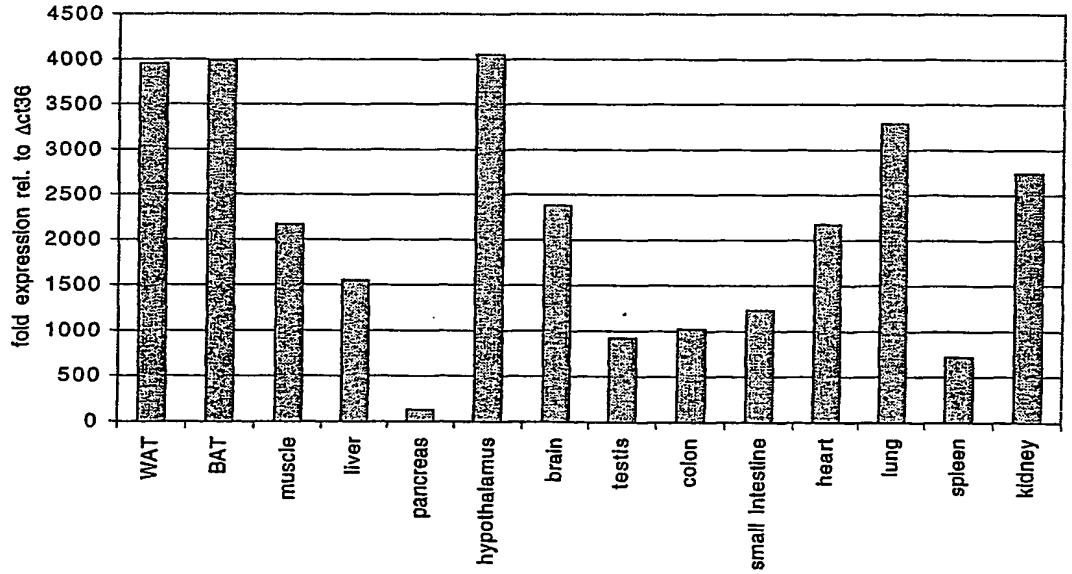

10/537798

Figure 22E. Real-time PCR analysis of Nr1d2 expression in different mouse models

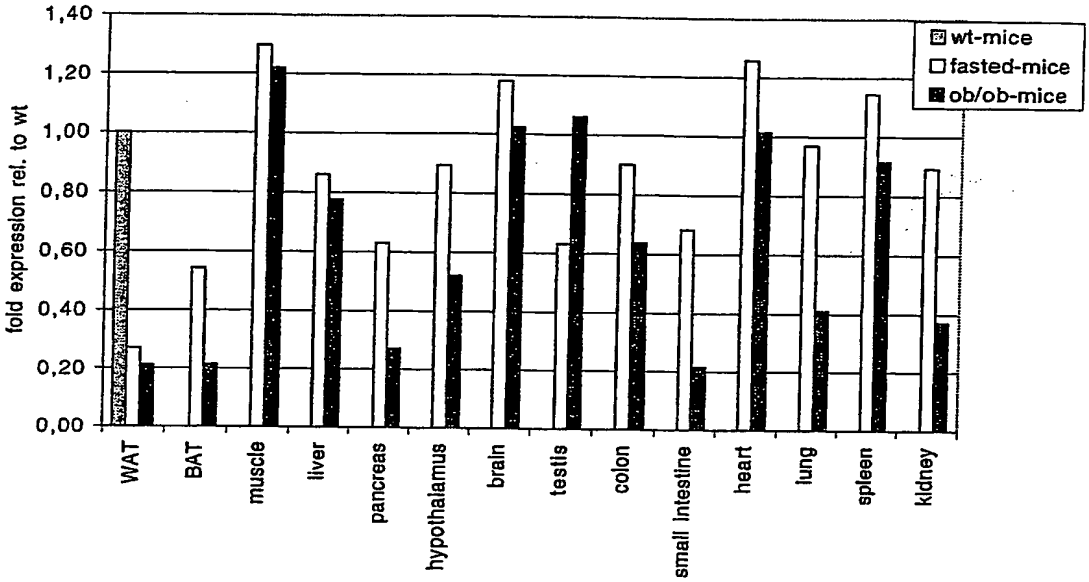

Figure 22F. Real-time PCR mediated analysis of Nr1d2 expression in 3T3-L1 cells differentiated from preadipocytes to mature adipocytes

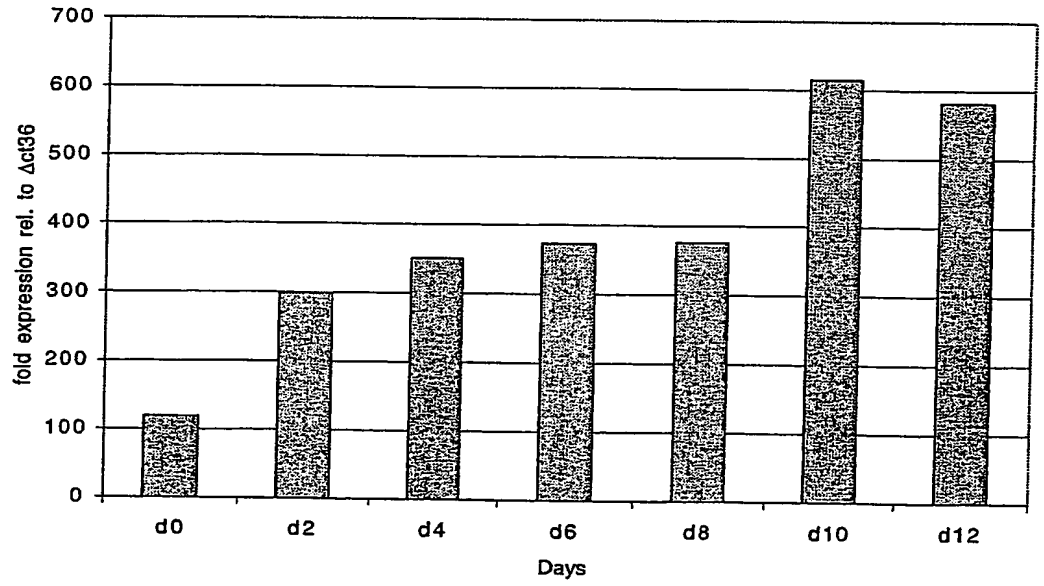

10/537798

Figure 23. Real-time PCR analysis of the expression of *Eip75B* homologs in different human tissues

Figure 23A. Real-time PCR analysis of NR1D1 expression in different human tissues

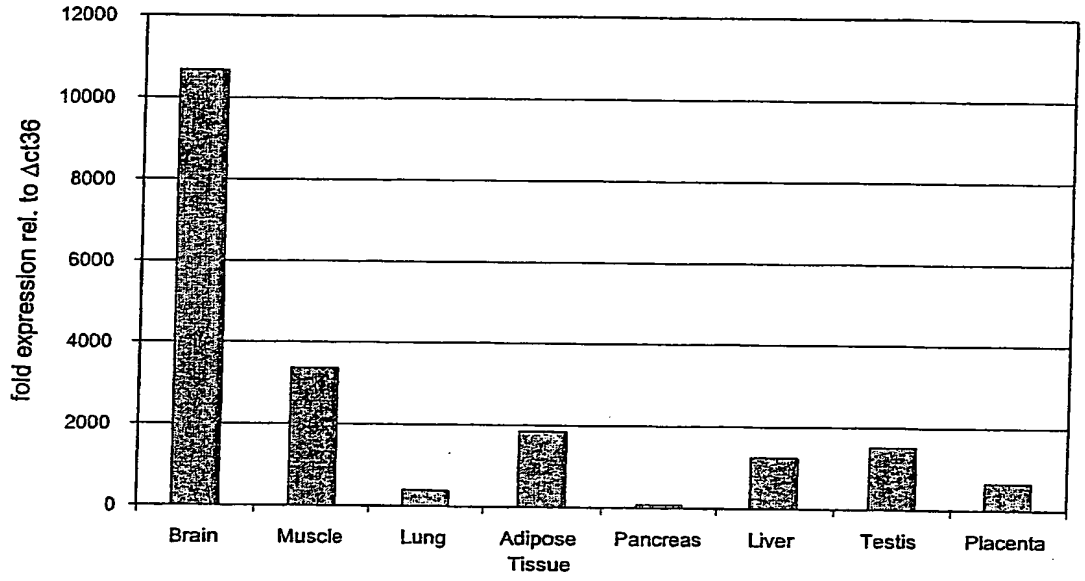

Figure 23B. Real-time PCR analysis of NR1D1 expression in different human adipose tissues

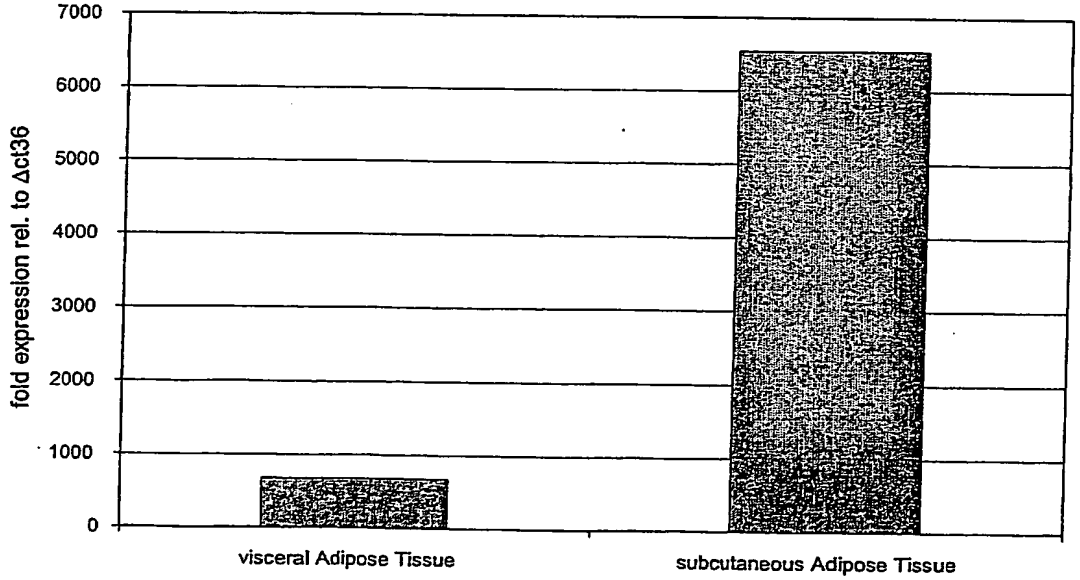

10/537798

Figure 23C. Real-time PCR analysis of NR1D1 expression in human abdominal derived primary adipocytes during preadipocyte differentiation

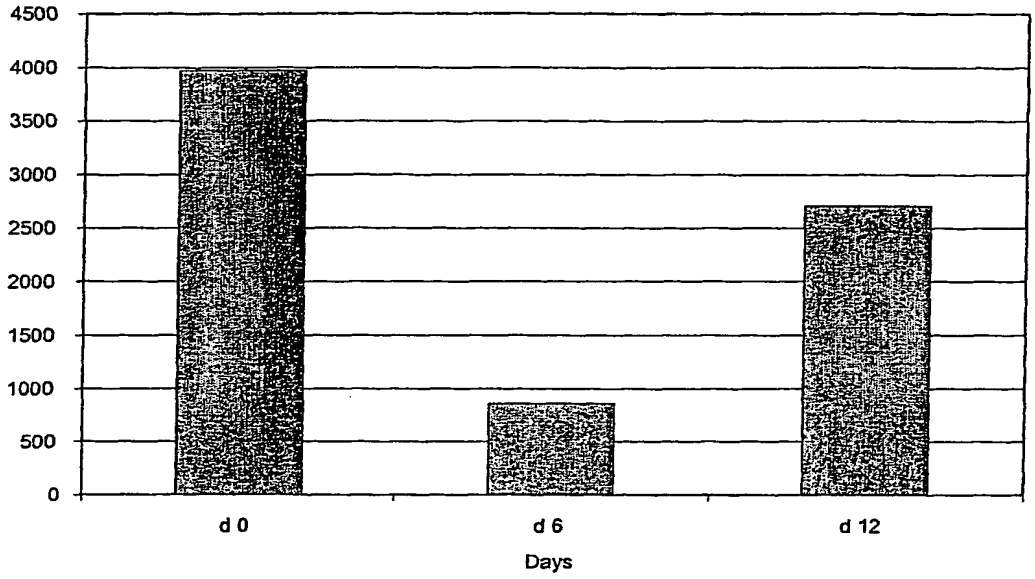

Figure 23D. Real-time PCR analysis of NR1D2 expression in different human tissues

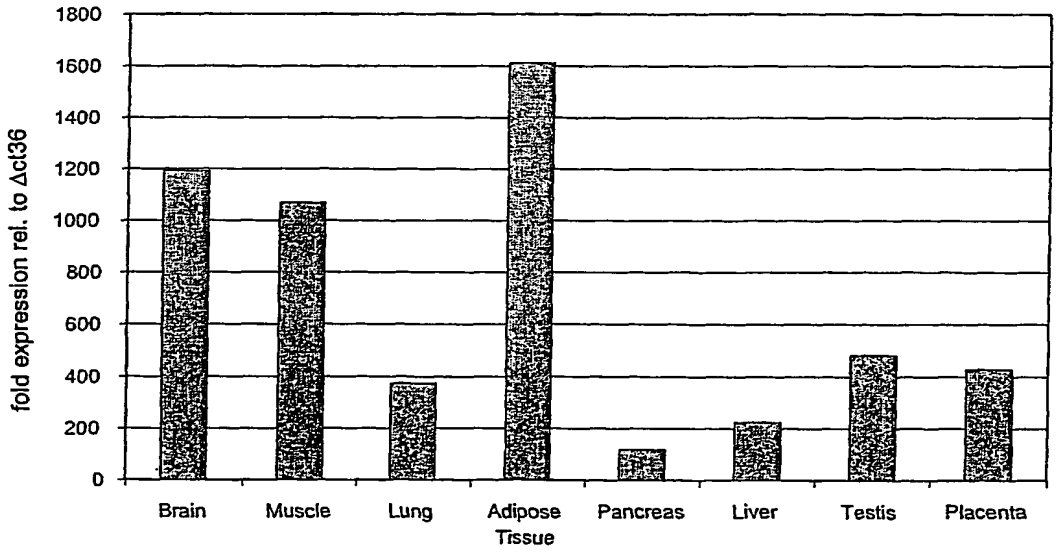

10/537798

Figure 23E. Real-time PCR analysis of NR1D2 expression in different human adipose tissues

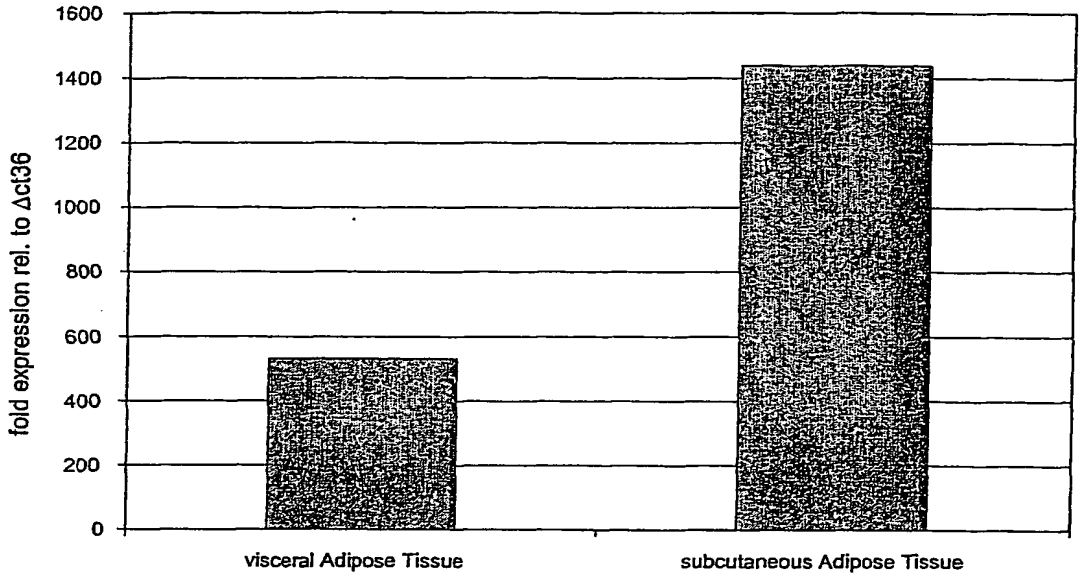

Figure 23F. Real-time PCR analysis of NR1D2 expression in human abdominal derived primary adipocytes during preadipocyte differentiation

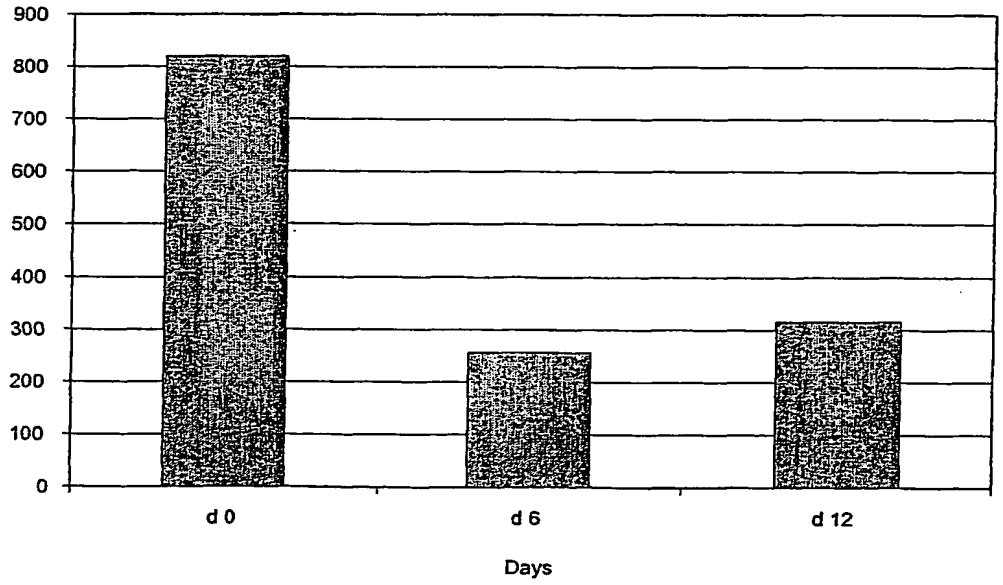

This Page is Inserted by IFW Indexing and Scanning Operations and is not part of the Official Record

BEST AVAILABLE IMAGES

Defective images within this document are accurate representations of the original documents submitted by the applicant.

Defects in the images include but are not limited to the items checked:

- ☐ BLACK BORDERS
- ☐ IMAGE CUT OFF AT TOP, BOTTOM OR SIDES
- ☐ FADED TEXT OR DRAWING
- ☑ BLURRED OR ILLEGIBLE TEXT OR DRAWING
- ☐ SKEWED/SLANTED IMAGES
- ☐ COLOR OR BLACK AND WHITE PHOTOGRAPHS
- ☐ GRAY SCALE DOCUMENTS
- ☐ LINES OR MARKS ON ORIGINAL DOCUMENT
- ☐ REFERENCE(S) OR EXHIBIT(S) SUBMITTED ARE POOR QUALITY
- ☐ OTHER: _____

IMAGES ARE BEST AVAILABLE COPY.
As rescanning these documents will not correct the image problems checked, please do not report these problems to the IFW Image Problem Mailbox.